Chromatographia (2017) 80:1371–1399
DOI 10.1007/s10337-017-3363-6

ORIGINAL

Analysis of NaoMaiTong Metabolites Using High-Performance Liquid Chromatography/High-Resolution Mass Spectrometry in Rat Urine

Xulei Fan[1] · Yueying Rong[1] · Shumei Wang[1]

Received: 29 April 2017 / Revised: 13 July 2017 / Accepted: 17 July 2017 / Published online: 29 July 2017

Abstract NaoMaiTong (NMT), consisting of *Radix et Rhizoma Rhei, Radix Ginseng*, *Radix Puerariae,* and *Rhizoma Ligustici Chuanxiong*, is widely used for treating ischemia cerebral apoplexy. In this work, a rapid high-performance liquid chromatograph coupled with a quadrupole-orbitrap mass spectrometer (HPLC-Q-Orbitrap) was developed for detection and identification of chemical compounds in rat urine after oral administration of NaoMaiTong and its single herbs. Using targeted screening and the mass defect filter of MetWorks™ software, a total of 157 ingredients were detected in the NaoMaiTong drug-containing group within 36 h, including 70 prototype chemicals and 61 related metabolites that were unambiguously discriminated. There were anthraquinones, triterpenoid saponins, isoflavones, puerosides, phthalides, phenolic acid, etc. Twelve triterpenoid saponins, including 7 metabolites, were first discovered in rat urine after administration. Mirificin-Glc and methoxypuerarin were first discovered in the *Radix Puerariae*. The results indicated that glucuronidation and sulfation were the main metabolic pathways of *Radix et Rhizoma Rhei* and *Radix Puerariae*. In addition to glucuronidation and sulfation, other conjugation reactions also occurred in the metabolisms of *Rhizoma Ligustici Chuanxiong* such as cysteine conjugation and acetylcysteine conjugation, while phase I reactions (e.g., deglycosylated, hydroxylated) were the major metabolic reaction for *Radix Ginseng*. Many compounds from its single herb-dosed groups presented different absorption trends and slower elimination rates in the urine from the NMT-dosed group compared with the urine from the single-dosed groups. These results will provide helpful information for further basic research into the active substances in NaoMaiTong.

Keywords HPLC-Q-Orbitrap · Metabolites · Metabolic pathways · NaoMaiTong

Introduction

NaoMaiTong (NMT), a traditional Chinese medicine prescription, was used by Professor JianSheng Li (Henan University of Traditional Chinese Medicine, China) during his decades of clinical experience in treating cerebral apoplexy. The recipe of NMT consists of four medicinal herbs, namely, *Radix et Rhizoma Rhei*, Panax ginseng C.A. Mey., *Pueraria lobata* (Willd.) Ohwi. and *Ligusticum chuanxiong Hort.* In the previous clinical studies, NMT had proved significantly protective and effective in treating cerebral ischemia–reperfusion injury [1–4]. NMT could reduce brain cell damage and improve the clinical symptoms, signs, and quality of life in patients with cerebral infarction [2]. A pharmacological study indicated that administration of the moderate dose of NMT (3.0 g/kg/day) for 5 days yielded effective protection [5]. A phytochemical investigation of the NMT formula denoted that its main constituents included anthraquinones, isoflavones, and triterpenoid saponins [6]. Related pharmacokinetic report provided the analysis of the chemical compounds in rat plasma samples after the oral administration of NMT [7, 8]. Although the pharmacological effects of NMT were investigated, the literature data on the metabolism of NMT decoction in rat urine are not available. To obtain extensive

Electronic supplementary material The online version of this article (doi:10.1007/s10337-017-3363-6) contains supplementary material, which is available to authorized users.

✉ Shumei Wang
2395903468@qq.com

[1] Guangdong Pharmaceutical University, Xiaoguwei Street, Panyu District, Guangzhou 510006, China

metabolism information for NMT decoction in rat urine, it is urgent to develop rapid and effective analytical methods for detection.

Recently, with the development of various data acquisition methods, liquid chromatography–mass spectrometry, especially high-resolution mass spectrometry (HRMS), has exhibited excellent performance in metabolite detection owing to its high resolution and accurate mass [9]. A high-performance liquid chromatograph coupled with a quadrupole-orbitrap mass spectrometer (HPLC-Q-Orbitrap), a rapid and sensitive technique with shorter analysis time and greater mass value accuracy, has widely been used to detect and identify the prototypes and metabolites in TCM [10]. HPLC-Q-Orbitrap combines high trapping capacity and the MS^n scanning function along with accurate mass measurements within 5 ppm and a resolving power of up to 100,000. Specifically, the orbitrap facilitates fast data-dependent acquisition of accurate MS^n spectra on an LC timescale, which could increase the throughput and identification efficiency for metabolites [11].

In the present study, we used a rapid and highly sensitive HPLC-Q-Orbitrap mass spectrometer to separate and detect chemical compounds in rat urine after oral administration of the NMT decoction and its individual herbs. With the aid of targeted screening and the mass defect filter of MetWorks™ software, background noise and endogenous ingredients can quickly be filtered, saving time using MetWorks software for rapid screening of metabolites. This study is the first to explain the NMT urine migration components to help in the study of NMT pharmacokinetics. The results could provide abundant chemical compound information for further pharmacology studies on NMT and lay the foundation for further elaboration of the compatibility principle of NMT.

Experimental Procedures

Chemicals and Reagents

HPLC-grade acetonitrile, methanol, and formic acid were purchased from Fisher (Fair Lawn, NJ, USA). Ultrapure water was prepared by a Millipore-Q water purification system (Bedford, MA, USA). Other reagents and chemicals were of analytical grade.

The reference standards of Aloe emodin, Rhein, Emodin, Puerarin, Daidzin, Ginsenoside Re, and Ferulic Acid were obtained from National Institute for the Control of Pharmaceutical and Biological Products (Beijing, China). The reference standards of ginsenoside Rc, ginsenoside Rf, ginsenoside Rg1, ginsenoside Rb2, ginsenoside Rb1, ginsenoside Rd, ginsenoside Rg3, ligustilide, and daidzein were purchased from Mansite Biotechnology Company (Chengdu, China). The reference standards of 3′-hydroxypuerarin, 3′-methoxypuerarin, physcion-8-*O*-Glc, chrysophanol-8-*O*-Glc, emodin8-*O*-Glc, rhein-8-*O*-Glc, senkyunolide I, senkyunolide A, butylphthalide, and aloe-emodin-8-*O*-Glc were obtained from Chroma Biotechnology Company (Chengdu, China).

Plant Material

Radix et Rhizoma Rhei, *Panax ginseng C.A.Mey.*, *Pueraria lobata (Willd.) Ohwi., and Ligusticum chuanxiong Hort.* were purchased from a Chinese herbal medicine market (Bozhou, Anhui, China), and were authenticated by the Chinese Pharmacopoeia content determination standard (ferulic acid content greater than 0.1%, puerarin content greater than 2.4%, the total content of ginsenoside Rg1 and ginsenoside Re more than 0.3%, ginsenoside Rb1 content more than 0.2%, and the total content of aloe emodin, rhein, emodin, chrysophanol, and physcion content more than 1.5%).

Preparation of NaoMaiTong

NMT consisting of *Radix et Rhizoma Rhei* (90 g), *Panax ginseng C.A. Mey.* (90 g), *Pueraria lobata* (*Willd.*) *Ohwi* (60 g) *and Ligusticum chuanxiong Hort.* (60 g) in a ratio of 9:9:6:6 by mass weight was immersed in a tenfold excess (based on mass weight) of 60% ethanol–water solution. The mixture was extracted by refluxing twice at 90 °C. The extracted solution was filtered. The two filtrates were combined and concentrated to 2 g sample drug per milliliter. The concentrated solutions of *Radix et Rhizoma Rhei, Panax ginseng C.A. Mey., Pueraria lobata (Willd.) Ohwi., and Ligusticum chuanxiong Hort.* were obtained in the same way. The extracted solutions of *Radix et Rhizoma Rhei* and *Panax ginseng C.A. Mey.* were concentrated to a concentration of 0.6 g sample drug per milliliter. The extracted solution of *Pueraria lobata (Willd.) Ohwi. and Ligusticum chuanxiong Hort.* was concentrated to 0.4 g sample drug per milliliter. The reference standards were dissolved in methanol.

Animal Experiments

Male Wistar rats (220–280 g) were purchased from Pengyue Experimental Animal Breeding Company (Jinan, China). The animals were bred in the Experimental Animal Center of Henan University of Traditional Chinese Medicine for 1 week before the experiment. The rats were randomly divided into six groups, six rats for each of the single-drug groups (Da-Huang, Ren-Shen, Ge-Gen, Chuan-Xiong), NMT groups, and a blank control group, respectively. The blank control group rats were orally administered ultrapure water. The compound control group, Da-Huang and Ren-Sheng Group, and Ge-Gen and Chuan-Xiong group

were exposed orally to the NMT preparation at a dose of 0.2 g·kg^{-1}, 0.06 g·kg^{-1}, and 0.04 g·kg^{-1}, respectively (the amount of the single-drug groups and single herb components of the compound control group in the amount of the same amount of medication). The rats were placed in metabolic cages to collect rat urine on the 5th day after the oral administration. The blank control group was collected during the 0–24 h period after oral administration. The drug-containing urine samples were collected during the 0–8, 8–12, 12–24, and 24–36 h periods. The urine samples were centrifuged at 1000 rpm for 30 min at 4 °C, and the supernatants were stored at −80 °C until analysis. All protocols and care of the rats were in accordance with the relevant national legislation and local guidelines.

Urine Sample Preparation

A solid-phase extraction (SPE) method was used to extract metabolites from the urine samples. The urine sample (1.0 mL) was added and flowed through LC-18 SPE columns (200 mg volume; Supelco, USA) using gravity. The SPE columns were washed with 3 mL ultrapure water, and then eluted with 3 mL 40% methanol, and 100% methanol, in turn. The eluants were merged and taken to dryness at 50 °C under a gentle stream of nitrogen gas. The residue was reconstituted with 400 µL 80% methanol (0.1% formic acid) and then centrifuged for 30 min at 1500 rpm at 4 °C. An aliquot of 10 µL of the supernatant was injected into the HPLC-Q-O-MS system for analysis.

LC–MS Analysis

The HPLC column was a Venusil XBP C18 chromatographic column (Agela Technologies, Tianjin, China). The mobile phase consisted of acetonitrile (A) and 0.1% formic acid in water (B).The gradient program was optimized as follows: 0–8 min: 10% A; 8–23 min: 10% A ~14% A; 23–43 min: 14%A ~20% A; 43–63 min: 20% A ~30% A; 63–68 min: 30% A ~35% A; 68–78 min: 35% A ~55% A; 78–82 min: 55% A ~70% A; 82–92 min: 70% A ~100% A; 92–102 min: 100% A ~10% A. The flow rate was maintained at 1 mL min^{-1}, and a post-column split was used to maintain a flow rate of 0.3 mL min^{-1} into the mass spectrometer source to obtain good nebulization efficiency.

A high-resolution Q-Exactive mass spectrometer (Thermo Fisher Scientific, Bremen, Germany), specifically a quadrupole-orbitrap hybrid mass spectrometer coupled with a heated electrospray ionization (HESI) source, was operated in both positive and negative ion modes. The mass conditions were as follows: auxiliary gas flow rate, 10.0 L min^{-1}; capillary temperature, 350 °C; spray voltage, 2.8 and 3.5 kV for the negative and positive modes, respectively; scan range, *m/z* 100–*m/z* 1500; stepped NCE, 20, 35 eV; auxiliary gas heater temperature, 200 °C. Q-Exactive 2.0 SP 2 (Thermo Fisher Scientific, USA) was used to control the mass spectrometer. XCalibur 3.0 software (Thermo Fisher Scientific, USA) was used to control the instrument and for data acquisition and analysis.

Data Analysis

In this study, LC/MS data from analysis of rat urine after oral administration of the NMT decoction and its individual herbs were processed using the MetWorks™ 1.3 SP4 software (Thermo Fisher Scientific, USA) component detection function. Phase I and II common factory lists offered by the MetWorks™ software. With the help of the mass defect filter, it was quick and convenient to filter background noise and endogenous ingredients to obtain potential active chemical ingredients from the NMT. The mass defect refers to the difference between the exact mass and integral mass of a compound or an ion. The method could automatically remove background interference and monitor the minor metabolites by setting the initial mass defect filtering algorithm [12–14]. Calculation of neutral losses between fragment ions and their elemental composition in the MS/MS spectrum of the candidates and comparisons with the fragment patterns of the parent chemical compounds showed that some candidates were possibly related to metabolites of NMT. The MS and MS/MS spectral data were used to identify both prototype and metabolite by offline data processing methods using the software Xcalibur™ 3.0 (Thermo Fisher Scientific, USA). The mass accuracy of the precursor ions was within ±5 ppm. The chemical structures of the metabolites detected were drawn by ChemBioDraw Ultra 13.0 (Cambridge, USA).

Results

Analysis of Components After Oral Administration of NMT in Rat Urine

The screening, identification, and further characterization of the metabolites of NMT in rat urine were first performed by HPLC-Q-Orbitrap in both the positive and negative ion modes. The basic chromatograms from the drug-containing urine at 90 min in the negative and positive mode are shown in Fig. 1a, b, respectively. The LC/MS chromatograms were compared between the blank group and the drug administration group; see Electronic Supplementary Material Fig. S1. The software Xcalibur™ 3.0 was used to compare the data of the blank group and the drug administration group. In total, 61 related metabolites that were identified or tentatively discriminated by comparing their MS data and retention times with those of reference compounds and single-drug groups or literature

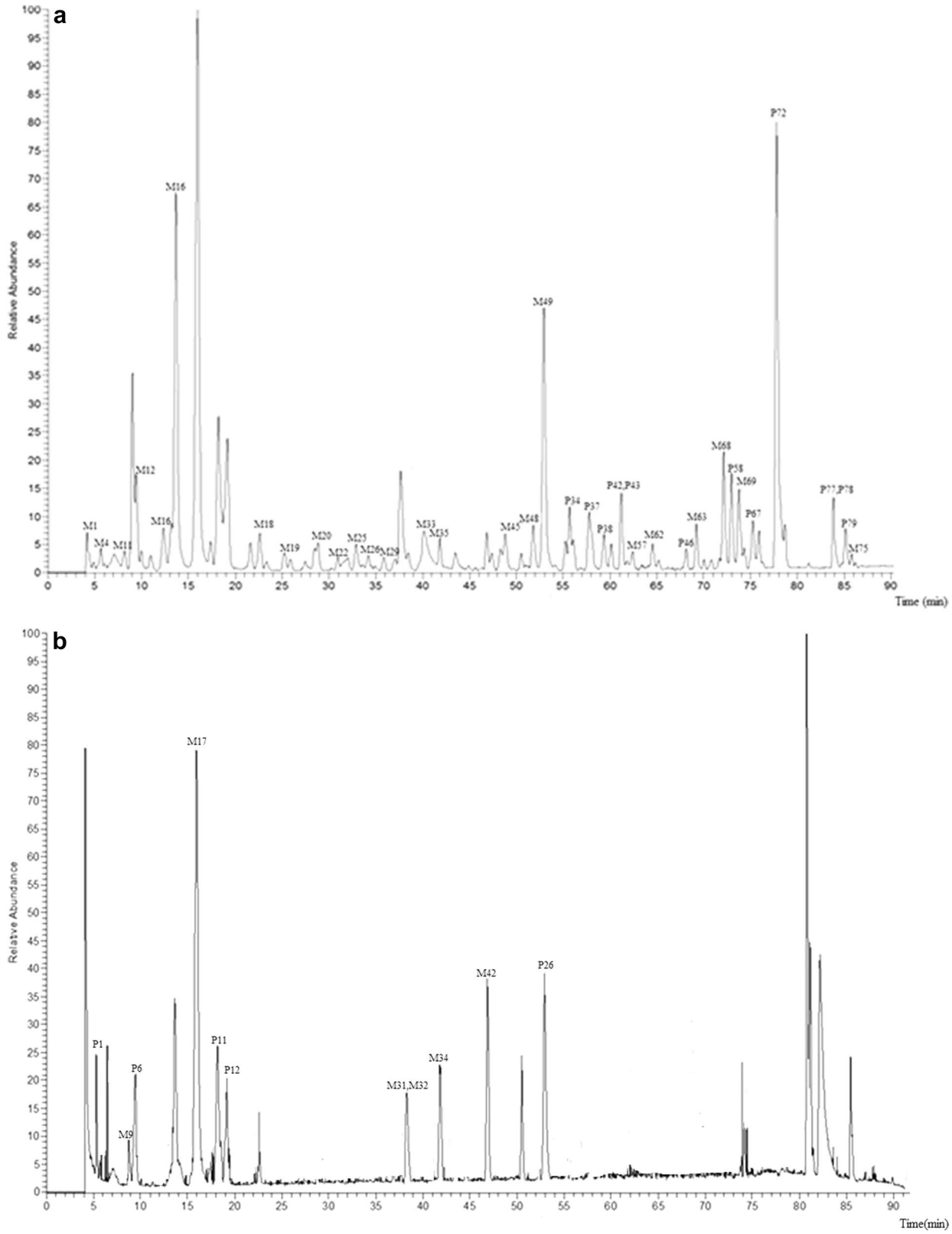

Fig. 1 **a** Base peak chromatograms of drug-containing urine at 90 min in negative mode. **b** Base peak chromatograms of drug-containing urine at 90 min in positive mode

data. Most chemical ingredients showed strong signals at 0–8 h and 8–12 h after oral administration. The metabolites of rhubarb and pueraria also displayed strong signals after 8–12 h. The chemical components were thinly transformed and removed from the body, and the signals detected with the mass detector, therefore, became weaker or vanished over time. In addition, 157 identified compounds, including their retention times, formulas, precursor ion MS/MS data, and metabolic pathway, etc., are shown in Table 1. Moreover, the origins of the discriminated components were confirmed by comparison of the MS data from single-drug-dosed groups with the data from the NMT-dosed group. The urine chromatograms of rats were measured at 8–12 h after administration. For urine chromatograms of the single-drug-dosed groups and the NMT dosed group see Electronic Supplementary Material Fig. S2.

Ingredients Derived from Radix et Rhizoma Rhei

The analysis of NMR data showed that the compounds of rhubarb were anthraquinones [15]; anthraquinone-related metabolites were formed through glucuronidation and sulfation, which were considered its metabolism pathways [16–21]. In addition, methylation and diglucuronidation conjugation were also found. For related metabolic pathways, see Electronic Supplementary Material Fig. S4. Most metabolites showed intense signals at 0–8 h in rat urine from the NMT-dosed group after administration. Interestingly, it can be detected after 8–12 h from rhubarb-dosed group. The results indicated that metabolites from rhubarb-dosed group were eliminated slowly.

Rhubarb anthraquinones had a common parent structure (1,8-dihydroxy-anthraquinone). Anthraquinone metabolites could be inferred from the characteristic fragments of the parent compound. For example, fragment ions at *m/z* 269.04 and 240.04 were inferred to be the relevant metabolites of aloe emodin (P70), fragment ions at *m/z* 253.05 and 225.05 as chrysophanol, fragments of *m/z* 269.04 and 225.05 were inferred to be emodin (P76), fragments of *m/z* 283.06 and 240.04 were inferred to be physcion, and fragments of *m/z* 283.02, 257.04 and 239.03 were inferred to be rhein (P72). Ultimately, five aloe emodin-related metabolites (M18, 23, 27, 36, and 38), four emodin-related metabolites (M41, 47, 58 and 66), five chrysophanol-related metabolites (M37, 40, 57, 59 and 62), two physcion-related metabolites (M63 and 65), four rhein-related metabolites (M25, 33, 44 and 69) were identified. In addition, 6-dehydroxylaccaic acid D-GlcA (M50) and catechin-GlcA (M6) were found in rat urine after administration.

Unfortunately, this identification method did not work for metabolites produced through a series of complicated metabolic pathway. M18, M23, and M27 displayed deprotonated ions $[M-H]^-$ at *m/z* 621.1104 corresponding to the molecular formula of $C_{27}H_{26}O_{17}$, 445.0778 corresponding to $C_{21}H_{18}O_{11}$, and 349.0025 corresponding to $C_{15}H_{10}O_8S$, respectively. The ions were 352 Da ($C_{12}H_{16}O_{12}$), 176 Da ($C_6H_8O_6$), and 80 Da (SO_3) higher than the ions of P70 (aloe emodin), respectively. Moreover, the ions all showed product ions at *m/z* 269.0454 and 240.0423 in the MS/MS spectra, which were similar to the ions of aloe emodin. Consequently, M18, M23, and M27 were tentatively identified as the diglucuronidated, glucuronidated, and sulfated metabolites of aloe emodin, respectively. However, their metabolic reaction site still needed further confirmation.

M25 and M33 yielded the $[M-H]^-$ ion at *m/z* 459.0574 ($C_{21}H_{16}O_{12}$) and 362.9821 ($C_{15}H_8O_9S$), respectively. The MS/MS spectra of M25, M33, and M69 exhibited fragment ions at *m/z* 257.0456 and 239.0346, which were similar to the ions of P72 (rhein). In addition, their molecular weights were 176 Da ($C_6H_8O_6$) and 80 Da (SO_3) higher than of the ions of P72. Therefore, this information indicated that M25 and M33 might be the glucuronidated and sulfated metabolites of rhein. However, the precise position of the glucuronidated and sulfated reaction sites could not be confirmed in this study.

Ingredients Derived from Panax Ginseng C.A. Mey

A total of 51 triterpenoid saponins, including 45 prototypes [18 protopanaxadiol (PPD) types, 9 protopanaxtriol (PPT) types, 6 oleanolic acid types, and 7 other types were shown in Fig S3] and 6 metabolites of unknown composition were found through a comparison with data obtained from the NMT extract. Although prototype components of saponins with abundant content were observed in the MS detector, their related metabolites were detected with very low levels. Moreover, the metabolites of triterpenoid saponins were detected in the urine from the NMT-dosed group at 0–8 h and declined quickly. However, these components in the urine from the ginseng-dosed group were rarely detected after 12 h. Deglycosylated, hydroxylated, and hydrogenated, hydrolyzed, etc. were the main metabolism pathways. PPD and PPT showed different fragment ions at *m/z* 459 and 475, respectively, whereas that at *m/z* 455 was identified as the oleanolic acid-type. Based on a preliminary summary of the different types of constituents with different mass defect filters, ginsenoside shortage in the negative mode quality range is of approximately 0.3–0.6 Da. In the MS^2 spectrum from the ginsenosides, continual losses of saccharide units were observed at high mass, and abundant fragments derived from the sugar units were detected at low mass [22, 23]. Therefore, from the above fragment pattern, ginsenosides were identified. For example, ions at *m/z* 179.06, 161.05, and 113.02 were derived from glucoside, *m/z* 145.05 and 163.06 came from rhamnoside, and *m/z* 131.04 and 149.05 came from xyloside or arabinose.

Based on exact masses, MS fragments and reference substance, P33–34, 49, 53–55, 58–61, 67, and

Table 1 Identified chemical compounds at different time points in rat urine after oral administration of NMT decoction

No.	Rt (min)	Identification	Formula molecular	Precursor ions (*m/z*)	Error (ppm)	MS/MS	Metabolic pathway	Resource
M1	4.74	Puerarin-sulfate	$C_{21}H_{20}O_{12}S$	495.0605 $[M-H]^-$	0.465	(−)415.1033 $[M-H-SO_3]^-$, 405.0288 $[M-H-C_3H_6O_3]^-$, 375.0184 $[M-H-C_4H_8O_4]^-$, 325.0718 $[M-H-SO_3-C_3H_6O_3]^-$, 295.0614 $[M-H-C_4H_8O_4]^-$	SUL	G
M2	4.91	3′-Hydroxypuerarin-*O*-GlcA	$C_{27}H_{28}O_{16}$	607.1287 $[M-H]^-$	−4.048	(−)431.0984 $[M-H-GlcA]^-$, 311.0566 $[M-H-GlcA-C_4H_8O_4]^-$, 283.0623 $[M-H-GlcA-C_5H_8O_5]^-$	GlcA	–
P1	5.11	3′-Hydroxypuerarin-*O*-Glc	$C_{27}H_{30}O_{15}$	595.1655 $[M+H]^+$	−0.414	(+)475.1227 $[M+H-C_4H_8O_4]^+$, 433.1227 $[M+H-Glc]^+$, 415.1018 $[M+H-Glc-H_2O]^+$, 313.0701 $[M+H-Glc-C_4H_8O_4]^+$, 283.0589 $[M+H-Glc-C_5H_{10}O_5]^+$	#	–
M3	5.48	Puerarin-*O*-GlcA	$C_{27}H_{28}O_{15}$	593.1497 $[M+H]^+$	−0.668	(+)417.1176 $[M+H-GlcA]^+$, 399.1071 $[M+H-GlcA-H_2O]^+$, 297.0754 $[M+H-GlcA-C_4H_8O_4]^+$, 267.0646 $[M+H-GlcA-C_5H_{10}O_5]^+$	GlcA	–
M4	5.62	3′-Hydroxypuerarin-*O*-sulfate	$C_{21}H_{20}O_{13}S$	511.0554 $[M-H]^-$	0.422	(−)431.0978 $[M-H-SO_3]^-$, 391.0128 $[M-H-C_4H_8O_4]^-$, 311.0565 $[M-H-SO_3-C_4H_8O_4]^-$, 283.0612 $[M+H-SO_3-C_5H_{10}O_5]^-$	SUL	–
P2	5.65	Puerarin-Glc	$C_{27}H_{30}O_{14}$	579.1704 $[M+H]^+$	−0.746	(+)459.1282 $[M+H-C_4H_8O_4]^+$, 417.1175 $[M+H-Glc]^+$, 399.1071 $[M+H-Glc-H_2O]^+$, 297.0753 $[M+H-Glc-C_4H_8O_4]^+$, 267.0638 $[M+H-Glc-C_5H_{10}O_5]^+$	#	G
M5	6.31	3′-Methoxypuerarin-GlcA	$C_{28}H_{30}O_{16}$	623.1605 $[M+H]^+$	−0.259	(+)447.1281 $[M+H-GlcA]^+$, 429.1177 $[M+H-GlcA-H_2O]^+$, 327.0858 $[M+H-GlcA-C_4H_8O_4]^+$, 297.0752 $[M+H-GlcA-C_5H_{10}O_5]^+$	GlcA	–

Table 1 (continued)

No.	Rt (min)	Identification	Formula molecular	Precursor ions (*m/z*)	Error (ppm)	MS/MS	Metabolic pathway	Resource
P3	6.42	Mirificin-Glc	$C_{32}H_{38}O_{18}$	711.2124 $[M+H]^+$	−0.971	(+)579.1706 $[M+H–Api]^+$, 561.1599 $[M+H–Api–H_2O]^+$, 459.1277 $[M+H–Api–C_4H_8O_4]^+$, 417.1176 $[M+H–Api–Glc]^+$, 399.1070 $[M+H–Api–Glc–H_2O]^+$, 297.0753 $[M+H–Api–Glc–C_4H_8O_4]^+$, 267.0647 $[M+H–Api–Glc–C_5H_{10}O_5]^+$	#	G
P4	6.53	3′-Methoxypuerarin-6″-*O*-Glc	$C_{28}H_{32}O_{15}$	607.1676 $[M-H]^-$	−3.053	(−)487.1248 $[M-H–C_4H_8O_4]^-$, 445.1102 $[M-H–Glc]^-$, 325.0708 $[M-H–Glc–C_4H_8O_4]^-$	#	G
M6	7.08	Catechin-GlcA	$C_{21}H_{22}O_{12}$	465.1039 $[M-H]^-$	0.109	(−)289.0720 $[M-H–GlcA]^-$, 245.0818 $[M-H–GlcA–CO_2]^-$, 205.0497 $[M-H–GlcA–C_4H_4O_2]^-$	GlcA	D
M7	7.76	3′-Hydroxypuerarin-GlcA	$C_{27}H_{28}O_{16}$	607.1309 $[M-H]^-$	0.728	(−)487.0893 $[M-H–C_4H_8O_4]^-$, 431.0983 $[M-H–GlcA]^-$, 341.0671 $[M-H–GlcA–C_3H_6O_3]^-$, 311.0565 $[M-H–GlcA–C_4H_8O_4]^-$	GlcA	G
M8	7.8	Ferulic acid-GlcA	$C_{16}H_{18}O_{10}$	369.0829 $[M-H]^-$	0.488	(−)193.0499 $[M-H–GlcA]^-$, 178.0263 $[M-H–GlcA–CH3]^-$, 149.0598 $[M-H–GlcA–CO_2]^-$	GlcA	C
M9	8.04	Puerarin-GlcA	$C_{27}H_{28}O_{15}$	593.1499 $[M+H]^+$	−0.331	(+)417.1175 $[M+H–GlcA]^+$, 399.1070 $[M+H–GlcA–2H_2O]^+$, 297.0754 $[M+H–GlcA–C_4H_8O_4]^+$, 267.0754 $[M+H–GlcA–C_5H_{10}O_5]^+$	GlcA	G
P5	8.17	Puerarin-Glc	$C_{27}H_{30}O_{14}$	579.1704 $[M+H]^+$	−0.746	(+)417.1173 $[M+H–Glc]^+$, 399.1068 $[M+H–Glc–H_2O]^+$, 297.0753 $[M+H–Glc–C_4H_8O_4]^+$, 267.0645 $[M+H–Glc–C_5H_{10}O_5]^+$	#	G
M10	8.45	Puerarin-sulfate	$C_{21}H_{20}O_{12}S$	495.0609 $[M-H]^-$	−1.254	(+)479.0628 $[M+H–H_2O]^+$, 417.1183 $[M+H–SO_3]^+$, 399.1071 $[M+H–SO_3–H_2O]^+$, 297.0753 $[M+H–SO_3–C_4H_8O_4]^+$, 267.0651 $[M+H–SO_3–C_5H_{10}O_5]^+$	SUL	G

Table 1 (continued)

No.	Rt (min)	Identification	Formula molecular	Precursor ions (*m/z*)	Error (ppm)	MS/MS	Metabolic pathway	Resource
M11	8.66	3′-Methoxypuerarin-sulfate	$C_{22}H_{22}O_{13}S$	525.0714 $[M-H]^-$	1.077	(−)445.1142 $[M-H-SO_3]^-$, 405.0281 $[M-H-C_4H_8O_4]^-$, 355.0829 $[M-H-SO_3-C_3H_6O_3]^-$, 325.0719 $[M-H-SO_3-C_4H_8O_4]^-$	SUL	G
M12	9.13	3′-Hydroxypuerarin-sulfate	$C_{21}H_{20}O_{13}S$	511.0553 $[M-H]^-$	0.226	(−)431.0985 $[M-H-SO_3]^-$, 391.0131 $[M-H-C_4H_8O_4]^-$, 341.0668 $[M-H-SO_3-C_3H_6O_3]^-$, 311.0565 $[M-H-SO_3-C_4H_8O_4]^-$, 283.0601 $[M-H-SO_3-C_5H_8O_5]^-$	SUL	G
P6	9.43	3′-Hydroxypuerarin*	$C_{21}H_{20}O_{10}$	433.1122 $[M+H]^+$	−1.67	(+)415.1017 $[M+H-H_2O]^+$, 313.0702 $[M+H-C_4H_8O_4]^+$, 283.0596 $[M+H-C_5H_{10}O_5]^+$	#	G
M13	9.59	3′-Methoxypuerarin-GlcA	$C_{28}H_{30}O_{16}$	621.1461 $[M-H]^-$	−1.013	(−)445.1140 $[M-H-GlcA]^-$, 431.0980 $[M-H-GlcA-CH2]^-$, 325.0722 $[M-H-GlcA-C_4H_8O_4]^-$, 311.0565 $[M-H-GlcA-CH2-C_4H_8O_4]^-$, 297.0786 $[M-H-GlcA-C_5H_8O_5]^-$	GlcA	G
P7	10.41	3′-Hydroxypuerarin-Xyl/ isomer	$C_{26}H_{28}O_{14}$	565.1548 $[M+H]^+$	−0.767	(+)433.1123 $[M+H-Xyl]^+$, 415.1013 $[M+H-Xyl-H_2O]^+$, 313.0702 $[M+H-Xyl-C_4H_8O_4]^+$, 283.0597 $[M+H-Xyl-C_5H_{10}O_5]^+$	#	G
M14	10.52	Puerarin-Xyl sulfate	$C_{22}H_{28}O_{21}$	627.1030 $[M-H]^-$	−3.238	(−)547.1459 $[M-H-SO_3]^-$, 375.0181 $[M-H-Xyl-C_4H_8O_4]^-$, 325.0720 $[M-H-SO_3-C_3H_6O_3]^-$, 295.0606 $[M-H-SO_3-C_4H_8O_4]^-$	SUL	G
P8	12.11	3′-Hydroxypuerarin-Xyl/ isomer	$C_{26}H_{28}O_{14}$	565.1547 $[M+H]^+$	−0.853	(+)433.1123 $[M+H-Api]^+$, 415.1019 $[M+H-Api-H_2O]^+$, 313.0702 $[M+H-Api\text{-}C_4H_8O_4]^+$, 283.0584 $[M+H-Api\text{-}C_5H_{10}O_5]^+$	#	G
M15	12.33	Ferulic acid-sulfate	$C_{10}H_{10}O_7S$	273.0076 $[M-H]^-$	0.562	(−)193.0498 $[M-H-SO_3]^-$, 178.0260 $[M-H-SO_3-CH3]^-$, 149.0595 $[M-H-SO_3-CO_2]^-$	SUL	C

Table 1 (continued)

No.	Rt (min)	Identification	Formula molecular	Precursor ions (*m/z*)	Error (ppm)	MS/MS	Metabolic pathway	Resource
M16	13.93	3′-Methoxypuerarin-GlcA	$C_{28}H_{30}O_{16}$	621.1464 $[M-H]^-$	0.47	(−)531.1140 $[M-H-C_3H_6O_3]^-$, 501.1038 $[M-H-C_4H_8O_4]^-$, 445.1139 $[M-H-GlcA]^-$, 417.1184 $[M-H-GlcA-CO]^-$, 355.0826 $[M-H-GlcA-C_3H_6O_3]^-$, 325.0719 $[M-H-GlcA-C_4H_8O_4]^-$	GlcA	G
M17	15.84	Unknown Cys	$C_{15}H_{25}O_5NS$	332.1521 $[M+H]^+$	−1.566	(+)315.1231 $[M+H-NH3]^+$, 314.1415 $[M+H-H_2O]^+$, 296.1309 $[M+H-2H_2O]^+$, 286.1467 $[M+H-CH_2O_2]^+$, 268.1361 $[M+H-CH4O3]^+$, 211.1320 $[M+H-Cys]^+$, 193.1222 $[M+H-Cys-H_2O]^+$, 175.1115 $[M+H-Cys-2H_2O]^+$, 165.1273 $[M+H-Cys-CH_2O_2]^+$	Cys	C
P9	15.95	Puerarin*	$C_{21}H_{20}O_9$	417.1175 $[M+H]^+$	−1.219	(+)399.1072 $[M+H-H_2O]^+$, 297.0755 $[M+H-C_4H_8O_4]^+$, 267.0652 $[M+H-C_5H_{10}O_5]^+$	#	G
P10	17.34	Puerarin-Xyl	$C_{26}H_{28}O_{13}$	549.1597 $[M+H]^+$	−0.835	(+)417.1175 $[M+H-Xyl]^+$, 399.1070 $[M+H-Xyl-H_2O]^+$, 297.0754 $[M+H-Xyl-C_4H_8O_4]^+$	#	G
P11	18.19	3′-Methoxypuerarin*	$C_{22}H_{22}O_{10}$	447.1282 $[M+H]^+$	−0.487	(+)429.1176 $[M+H-H_2O]^+$, 327.0858 $[M+H-C_4H_8O_4]^+$, 297.0753 $[M+H-C_5H_{10}O_5]^+$	#	G
P12	19.17	Puerarin-Api	$C_{26}H_{28}O_{13}$	549.1600 $[M+H]^+$	−0.487	(+)417.1175 $[M+H-Api]^+$, 399.1070 $[M+H-Api-H_2O]^+$, 297.0755 $[M+H-Api-C_4H_8O_4]^+$, 267.0648 $[M+H-Api-C_5H_{10}O_5]^+$	#	G
P13	21.16	3′-Methoxypuerarin-Api	$C_{27}H_{30}O_{14}$	579.1705 $[M+H]^+$	−0.573	(+)447.1281 $[M+H-Api]^+$, 429.1176 $[M+H-Api-H_2O]^+$, 327.0858 $[M+H-Api-C_4H_8O_4]^+$, 297.0753 $[M+H-Api-C_5H_{10}O_5]^+$	#	G
M18	22.01	Aloe-emodin-diGlcA	$C_{27}H_{26}O_{17}$	621.1104 $[M-H]^-$	1.091	(−)445.0778 $[M-H-GlcA]^-$, 269.0456 $[M-H-2GlcA]^-$, 253.0508 $[M-H-2GlcA-O]^-$	diGlcA	D
M19	25.74	Biochanin A-GlcA	$C_{22}H_{20}O_{11}$	459.0938 $[M-H]^-$	1.123	(−)283.0612 $[M-H-GlcA]^-$, 268.0384 $[M-H-GlcA-CH3]^-$	GlcA	G

Table 1 (continued)

No.	Rt (min)	Identification	Formula molecular	Precursor ions (*m/z*)	Error (ppm)	MS/MS	Metabolic pathway	Resource
P14	25.83	Genistein-8-C–Glc-Api/isomer	$C_{26}H_{28}O_{14}$	565.1545 $[M+H]^+$	−1.207	(+)433.124 $[M+H–Api]^+$, 415.1017 $[M+H–Api–H_2O]^+$, 313.0701 $[M+H–Api\text{-}C_4H_8O_4]^+$, 283.0594 $[M+H–Api–C_5H_{10}O_5]^+$	#	G
P15	26.46	Methoxypuerarin	$C_{22}H_{22}O_{10}$	447.1288 $[M+H]^+$	0.507	(+)429.1180 $[M+H–H_2O]^+$, 327.0860 $[M+H–C_4H_8O_4]^+$, 297.0754 $[M+H–C_5H_{10}O_5]^+$, 271.0595 $[M+H–Glc–CH_2]^+$	#	G
P16	27.45	Unknown	$C_{21}H_{20}O_{10}$	431.0986 $[M-H]^-$ 433.1123 $[M+H]^+$	0.534	(−)311.0565 $[M–H–C_4H_8O_4]^-$, 283.0611 $[M-H–C_5H_8O_5]^-$, 255.0666 $[M-H–C_6H_8O_6]^-$	#	G
P17	28.44	Ferulic acid*	$C_{10}H_{10}O_4$	195.0651 $[M+H]^+$	−0.437	(+)177.0544 $[M+H-H_2O]^+$, 163.0387, 145.0282 $[M+H–CH4O]^+$	#	C
P18	28.85	Genistein-8-C–Glc-Api/isomer	$C_{26}H_{28}O_{14}$	565.1546 $[M+H]^+$	−1.03	(+)433.1122 $[M+H–Api]^+$, 415.1017 $[M+H–Api–H_2O]^+$, 313.0701 $[M+H–Api–C_4H_8O_4]^+$, 283.0593 $[M+H–Api–C_5H_{10}O_5]^+$	#	G
M20	29.14	Puerol A-GlcA	$C_{23}H_{22}O_{11}$	473.1094 $[M-H]^-$	0, 984	(−)297.0768 $[M–H–GlcA]^-$, 253.0869 $[M-H–GlcA–CO_2]^-$, 190.9277, 175.0240 $[GlcA–H]^-$	GlcA	G
M21	29.51	Methoxygenistein-8-C–Glc	$C_{22}H_{22}O_{11}$	463.1230 $[M+H]^+$	−1.053	(+)445.1125 $[M+H–H_2O]^+$, 367.0807 $[M+H–C_2H8O4]^+$, 343.0807 $[M+H–C_4H_8O_4]^+$, 313.0697 $[M+H–C_5H_{10}O_5]^+$	Methoxy	G
M22	30.58	25-Hydroxyl-PPT-*O*-diGlc	$C_{42}H_{74}O_{15}$	863.5018 $[M+HCOO]^-$	0.957	(−)655.4409 $[M–H–Glc]^-$, 493.3886 $[M-H–2Glc]^-$	Hydrolysis+deGlc	R
P19	31.49	Pueroside A	$C_{29}H_{34}O_{14}$	605.1881 $[M-H]^-$	2.674	(−)297.0768 $[M–H–GlcA–Rha]^-$, 267.0666 $[M-H–GlcA–RhA–CH_2O]^-$, 253.0869 $[M-H–GlcA–RhA–CO_2]^-$	#	G
M23	31.69	Aloe-emodin-GlcA	$C_21H_{18}O_{11}$	445.0778 $[M-H]^-$	0.372	(−)269.0457 $[M–H–GlcA]^-$, 240.0424 $[M-H–GlcA–CHO]^-$	GlcA	D

Table 1 (continued)

No.	Rt (min)	Identification	Formula molecular	Precursor ions (*m/z*)	Error (ppm)	MS/MS	Metabolic pathway	Resource
M24	31.98	Senkyunolide J/N-GlcA	$C_{18}H_{26}O_{10}$	403.1595 $[M+H]^+$	−0.926	(+)229.0854 $[M+H–C_{11}H_{10}O_2]^+$, 227.1276 $[M+H–GlcA]^+$, 209.1170 $[M+H–C_6H_{10}O_7]^+$, 191.1064 $[M+H–GlcA–2H_2O]^+$, 163.1116 $[M+H–GlcA–CH_4O_3]^+$	GlcA	C
M25	32.90	Rhein-GlcA	$C_{21}H_{16}O_{12}$	459.0574 $[M-H]^-$	1.091	(−)283.0249 $[M-H–GlcA]^-$, 257.0450 $[M-H–GlcA–CO+2H]^-$, 239.0346 $[M-H–GlcA–CO_2]^-$	GlcA	D
M26	34.09	Senkyunolide F-GlcA	$C_{18}H_{22}O_9$	381.1193 $[M-H]^-$	0.511	(−)205.0863 $[M-H–GlcA]^-$, 187.0755 $[M-H–GlcA–H_2O]^-$	GlcA	C
M27	34.71	Aloe-emodin-sulfate	$C_{15}H_{10}O_8S$	349.0025 $[M-H]^-$	0.398	(−)269.0456 $[M-H–SO_3]^-$, 240.0421 $[M-H–SO_3–CHO]^-$	SUL	D
P20	35.71	Senkyunolide K/G	$C_{12}H_{16}O_3$	209.1170 $[M+H]^+$	−1.056	(+)191.1064 $[M+H–H_2O]^+$, 163.1115 $[M+H–C_2H6O]^+$	#	C
M28	35.84	Senkyunolide J/N-GlcA	$C_{18}H_{26}O_{10}$	403.1592 $[M+H]^+$	−1.67	(+)227.1274 $[M+H–GlcA]^+$, 209.1170 $[M+H–GlcA–H_2O]^+$, 191.1064 $[M+H–GlcA\text{-}2H_2O]^+$, 163.1114 $[M+H–GlcA–CH_4O_3]^+$	GlcA	C
M29	36.11	Puerol A-GlcA	$C_{23}H_{22}O_{11}$	473.1092 $[M-H]^-$	0.561	(−)297.0769 $[M-H–GlcA]^-$, 253.0869 $[M-H–GlcA–CO_2]^-$	GlcA	G
M30	37.69	Genistein-sulfate	$C_{15}H_{10}O_8S$	349.0023 $[M-H]^-$	−0.175	(−)269.0457 $[M-H–SO_3]^-$, 242.0585 $[M-SO_3–CO]^-$	SUL	G
M31	38.17	Senkyunolide J/N cysteine	$C_{15}H_{23}O_5NS$	330.1366 $[M+H]^+$	−1.121	(+)313.1093 $[M+H–NH_3]^+$, 284.1310 $[M+H–CH_2O_2]^+$, 209.1170 $[M+H–Cys]^+$, 191.1064 $[M+H–Cys–H_2O]^+$, 163.1114 $[M+H–Cys–CH_2O_2]^+$, 153.0544 $[M+H–Cys–C_4H_8]^+$	Cys	C
M32	38.23	Methoxydaidzein sulfate	$C_{16}H_{12}O_8S$	365.0322 $[M+H]^+$	−0.999	(+)285.0753 $[M+H–SO_3]^+$, 270.0516 $[M+H–SO_3–CH_3]^+$, 253.0487 $[M+H–SO_3–CH_4O]^+$	SUL	G

Table 1 (continued)

No.	Rt (min)	Identification	Formula molecular	Precursor ions (*m/z*)	Error (ppm)	MS/MS	Metabolic pathway	Resource
P21	38.81	Formononetin 8-C–Glc-Xyl	$C_{27}H_{30}O_{13}$	563.1753 $[M+H]^+$	−1.096	(+)431.1331 $[M+H–Xyl]^+$, 413.1225 $[M+H–Xyl–H_2O]^+$, 311.0909 $[M+H–Xyl–C_4H_8O_4]^+$, 281.0800 $[M+H–Xyl–C_5H_{10}O_5]^+$	#	G
M33	40.14	Rhein-sufate	$C_{15}H_8O_9S$	362.9821 $[M-H]^-$	1.307	(−)283.0250 $[M-H–SO_3]^-$, 268.0378 $[M-H–SO_3–CH3]^-$, 257.0448 $[M-H–SO_3–CO+2H]^-$, 239.0343 $[M-H–SO_3–CO_2]^-$	SUL	D
P22	40.26	Formononetin 8-C–Glc-Api	$C_{27}H_{30}O_{13}$	563.1751 $[M+H]^+$	−1.451	(+)431.1329 $[M+H–Api]^+$, 413.1223 $[M+H–Api–H_2O]^+$, 311.0907 $[M+H–Api–C_4H_8O_4]^+$, 281.0796 $[M+H–Api–C_5H_{10}O_5]^+$	#	G
M34	41.78	Senkyunolide J/N cysteine	$C_{15}H_{23}O_5NS$	330.1367 $[M+H]^+$	2.549	(+)313.1099 $[M+H–NH3]^+$, 284.1312 $[M+H–CH_2O_2]^+$, 209.1171 $[M+H–Cys]^+$, 191.1065 $[M+H–Cys–H_2O]^+$, 163.1116 $[M+H–Cys–CH_2O_2]^+$	Cys	–
M35	42.58	Biochanin A-GlcA	$C_{22}H_{20}O_{11}$	459.0938 $[M-H]^-$	1.123	(−)283.0608 $[M-H–GlcA]^-$, 268.0378 $[M-H–GlcA–CH_3]^-$, 239.0343 $[M-H–GlcA–C_2H_4O]^-$	GlcA	G
M36	44.10	Aloe-emodin-GlcA	$C_{21}H_{18}O_{11}$	445.0779 $[M-H]^-$	1.788	(−)269.0456 $[M-H–GlcA]^-$, 240.0425 $[M-H–GlcA–CHO]^-$	GlcA	D
M37	44.10	Chrysophanol-diGlcA	$C_{27}H_{28}O_{15}$	591.1366 $[M-H]^-$	4.681	(−)429.0841 $[M-H–Glc]^-$, 253.0508 $[M-H–GlC–GlcA]^-$	GlcA	D
M38	44.14	Aloe emodin-sulfate	$C_{15}H_{10}O_8S$	349.0026 $[M-H]^-$	0.684	(−)269.0456 $[M-H–SO_3]^-$, 240.0421 $[M-H–SO_3–CHO]^-$	SUL	D
M39	44.47	Senkyunolide I cysteine	$C_{15}H_{21}O_5NS$	328.1211 $[M+H]^+$	−0.67	(+)282.1154 $[M+H–CH_2O_2]^+$, 207.1014 $[M+H–Cys]^+$, 189.0910 $[M+H–Cys–H_2O]^+$, 165.0907 $[M+H–Cys–C_2H_2O]^+$	Cys	C
M40	46.14	Chrysophanol-diGlcA	$C_{27}H_{26}O_{16}$	605.1156 $[M-H]^-$	1.309	(−)429.0856 $[M-H–GlcA]^-$, 253.0504 $[M-H–2GlcA]^-$	diGlcA	D

Table 1 (continued)

No.	Rt (min)	Identification	Formula molecular	Precursor ions (*m/z*)	Error (ppm)	MS/MS	Metabolic pathway	Resource
M41	46.59	Emodin-diGlcA	$C_{27}H_{26}O_{17}$	621.1101 $[M-H]^-$	0.608	(−)445.0777 $[M-H-GlcA]^-$, 269.0456 $[M-H-2GlcA]^-$, 241.0440 $[M-H-2GlcA-CO]^-$	diGlcA	D
M42	47.46	Unknown Cys	$C_{15}H_{25}O_5NS$	332.1521 $[M+H]^+$	−1.566	(+)315.1254 $[M+H-NH_3]^+$, 286.1467 $[M+H-CH_2O_2]^+$, 211.1326 $[M+H-Cys]^+$, 193.1221 $[M+H-Cys-H_2O]^+$, 175.1120 $[M+H-Cys-2H_2O]^+$, 163.1272 $[M+H-Cys-CH_2O_2]^+$	Cys	–
M43	48.65	Unknown sulfate	$C_{12}H_{14}O_7S$	303.0530 $[M+H]^+$	−0.99	(+)285.0423 $[M+H-H_2O]^+$, 205.0857 $[M+H-H_2O\text{-}SO_3]^+$, 187.0751 $[M+H-2H_2O\text{-}SO_3]^+$, 177.0907 $[M+H-2H_2O-SO_3-CO]^+$	Hydrolysis+SUL	C
M44	48.78	Rhein-GlcA	$C_{21}H_{16}O_{12}$	459.0574 $[M-H]^-$	1.091	(−)283.0250 $[M-H-GlcA]^-$, 257.0456 $[M-H-GlcA-CO]^-$, 239.0346 $[M-H-GlcA-CO_2]^-$	GlcA	D
M45	49.35	3-Butyl-4-hydroxyphthalide-GlcA	$C_{18}H_{22}O_9$	383.1333 $[M+H]^+$	−0.963	(+)207.1014 $[M+H-GlcA]^+$, 189.0908 $[M+H-GlcA-H_2O]^+$, 161.0959 $[M+H-GlcA-CH_2O_2]^+$, 151.0389 $[M+H-GlcA-C_4H_8]^+$	GlcA	C
–	49.56	Unknown	$C_{17}H_{14}O5$	299.0911 $[M+H]^+$	−1.003	(+)281.0804 $[M+H-H_2O]^+$, 253.0856 $[M+H-CH_2O_2]^+$, 239.0700 $[M+H-C_2H_4O_2]^+$	–	G
M46	50.10	Unknown NAcCys	$C_{17}H_{25}O_7NS$	386.1280 $[M-H]^-$	0.269	(−)257.0851 $[M-H-C_5H_7O_3N]^-$, 239.0742 $[M-H-C_5H_7O_3N-H_2O]^-$, 223.0972 $[M-H-NAcCys]^-$	NAcCys	C
M47	50.34	Emodin-GlcA	$C_{21}H_{18}O_{11}$	445.0780 $[M-H]^-$	0.821	(−)269.0456 $[M-H-GlcA]^-$, 225.0551 $[M-H-GlcA-CO_2]^-$	GlcA	D
P23	50.81	Sophoraside A	$C_{24}H_{26}O_{10}$	473.1458 $[M-H]^-$	3.332	(−)311.0928 $[M-H-Glc]^-$, 267.1028 $[M-H-Glc-CO_2]^-$, 252.0790 $[M-H-Glc-C_2H_3O_2]^-$	#	G

Table 1 (continued)

No.	Rt (min)	Identification	Formula molecular	Precursor ions (*m/z*)	Error (ppm)	MS/MS	Metabolic pathway	Resource
P24	50.96	Unknown G	$C_{50}H_{92}O_{31}$	616.2760 $[M+CO_2]^{2-}$	−0.958	(−)1187.5530 $[M-H]^-$, 1025.4994 $[M-H-Glc]^-$, 863.4499 $[M-H-2Glc]^-$, 683.3821 $[M-H-3Glc-H_2O]^-$	#	R
M48	51.34	Unknown sulfate	$C_{13}H_{16}O_8S$	331.0497 $[M-H]^-$	1.174	(−)251.0923 $[M-H-SO_3]^-$, 236.0686 $[M-H-SO_3-CH_3]^-$, 207.1009 $[M-H-SO_3-CO_2]^-$, 192.0782 $[M-H-SO_3-C_2H_3O_2]^-$	SUL	C
–	51.49	Unknown	$C_{12}H_{12}O_2$	189.0909 $[M+H]^+$	−0.562	(+)171.0802 $[M+H-H_2O]^+$, 161.0959 $[M+H-CO]^+$, 143.0854 $[M+H-CO_2]^+$	–	C
P25	51.83	20-GlC–G Rf	$C_{48}H_{82}O_{19}$	1007.5437 $[M+HCOO]^-$	0.464	(−)961.5384 $[M-H]^-$, 799.4843 $[M-H-Glc]^-$, 637.4306 $[M-H-2Glc]^-$, 475.3785 $[M-H-3Glc]^-$	#	R
M49	52.38	Puerol B-GlcA	$C_{24}H_{24}O_{11}$	487.1250 $[M-H]^-$	0.853	(−)311.0928 $[M-H-GlcA]^-$, 267.1028 $[M-H-GlcA-CO_2]^-$, 252.0789 $[M-H-GlcA-C_2H_3O_2]^-$	GlcA	G
P26	52.94	Daidzein*	$C_{15}H_{10}O_4$	255.0649 $[M+H]^+$	−1.119	(+)255.0648 $[M+H]^+$	#	G
P27	53.16	N R1/isomer	$C_{47}H_{80}O_{18}$	977.5326 $[M+HCOO]^-$	−0.069	(−)931.5280 $[M-H]^-$, 799.4857 $[M-H-Xyl]^-$, 769.4740 $[M-H-Glc]^-$, 637.4326 $[M-H-Xyl-Glc]^-$, 475.3793 $[M-H-Xyl-2Glc]^-$	#	R
P28	53.33	Dihydroxyginsenoside Rb1 (Quinquenoside L16)	$C_{54}H_{94}O_{25}$	616.3028 $[M+2HCOO]^{2-}$	0.63	(−)1141.6057 $[M-H]^-$, 979.5461 $[M-H-Glc]^-$, 817.4984 $[M-H-2Glc]^-$, 799.4843 $[M-H-2Glc-H_2O]^-$, 655.4457 $[M-H-3Glc]^-$	#	R
P29	53.48	Isoswertisin 2″-*O*-xyloside	$C_{27}H_{30}O_{14}$	579.1705 $[M+H]^+$	−0.573	(+)447.1278 $[M+H-C_5H_8O_4]^+$, 429.1174 $[M+H-C_5H_8O_4-H_2O]^+$, 411.1070 $[M+H-C_5H_8O_4-2H_2O]^+$, 327.0857 $[M+H-C_5H_8O_4-C_4H_8O_4]^+$, 297.0753 $[M+H-C_5H_8O_4-C_5H_{10}O_5]^+$, 285.0742 $[M+H-C_5H_8O_4-Glc]^+$	#	–

Table 1 (continued)

No.	Rt (min)	Identification	Formula molecular	Precursor ions (*m/z*)	Error (ppm)	MS/MS	Metabolic pathway	Resource
P30	53.88	Chikusetsusaponin FM1/ isomer	$C_{53}H_{92}O_{24}$	601.2981 $[M+2HCOO]^{2-}$	1.614	(−)1111.5892 $[M-H]^-$, 997.5048, 979.5576 $[M-H-Xyl/Api]^-$, 817.4963 $[M-H-Xyl/Api-Glc]^-$, 799.4853 $[M-H-Xyl/Api\text{-}Glc-H_2O]^-$, 655.4378 $[M-H-Xyl/Api-2Glc]^-$	#	R
M50	54.15	6-Dehydroxylaccaic acid D-GlcA	$C_{22}H_{18}O_{12}$	473.0730 $[M-H]^-$	0.953	(−)297.0405 $[M-H-GlcA]^-$, 267.1028, 253.0505 $[M-H-GlcA-CO_2]^-$	GlcA	D
P31	55.17	Chikusetsusaponin FM1/ isomer	$C_{53}H_{92}O_{24}$	601.2977 $[M+2HCOO]^{2-}$	0.949	(−)1111.5879 $[M-H]^-$, 817.4936 $[M-H-Xyl/Api-Glc]^-$, 799.4850 $[M-H-Xyl/Api-Glc-H_2O]^-$	#	R
M51	55.23	Puerol B-GlcA	$C_{24}H_{24}O_{11}$	487.1248 $[M-H]^-$	0.442	(−)311.0927 $[M-H-GlcA]^-$, 267.1027 $[M-H-GlcA-CO_2]^-$, 252.0791 $[M-H-GlcA-C_2H_3O_2]^-$	GlcA	G
M52	55.26	Unknown NAcCys	$C_{17}H_{27}O_6NS$	374.1629 $[M+H]^+$	−0.761	(+)332.1525 $[M+H-C_2H_2O]^+$, 328.1574 $[M+H-CH_2O_2]^+$, 315.1249 $[M+H-C_2H_5NO]^+$, 286.1469 $[M+H-C_6H_2N]^+$, 268.1361 $[M+H-C_6H_2NO]^+$, 251.1089 $[M+H-C_3H_9NO_4]^+$, 211.1327 $[M+H-NAcCys]^+$, 193.1223 $[M+H-C_5H_9O_3NS-H_2O]^+$	NAcCys	C
P32	55.61	Dihydroxyginsenoside Rb1(Quinquenoside L16)	$C_{54}H_{94}O_{25}$	616.3026 $[M+2HCOO]^{2-}$	0.306	(−)1141.6064 $[M-H]^-$, 979.5479 $[M-H-Glc]^-$, 817.4962 $[M-H-2Glc]^-$, 799.4852 $[M-H-2Glc-H_2O]^-$, 655.4421 $[M-H-3Glc]^-$, 493.3883 $[M-H-4Glc]^-$	#	R
P33	55.68	G Rg1*	$C_{42}H_{72}O_{14}$	845.4907 $[M+HCOO]^-$	0.344	(−)799.4864 $[M-H]^-$, 637.4327 $[M-H-Glc]^-$, 475.3792 $[M-H-2Glc]^-$	#	R
P34	56.05	G Re*	$C_{48}H_{82}O_{18}$	991.5487 $[M+HCOO]^-$	0.385	(−)945.5434 $[M-H]^-$, 799.4845 $[M-H-Rha]^-$, 783.4905 $[M-H-Glc]^-$, 637.4341 $[M-H-Glc-Rha]^-$, 475.3797 $[M-H-2Glc-Rha]^-$	#	R

Table 1 (continued)

No.	Rt (min)	Identification	Formula molecular	Precursor ions (*m/z*)	Error (ppm)	MS/MS	Metabolic pathway	Resource
P35	56.64	Chikusetsusaponin FM1/ isomer	$C_{53}H_{92}O_{24}$	601.2978 $[M+2HCOO]^{2-}$	1.116	(−)1111.5913 $[M-H]^-$, 817.4956 $[M-H-Xyl/Api-Glc]^-$, 799.4841 $[M-H-Xyl/Api-Glc-H_2O]^-$, 637.4319 $[M-H-Xyl/Api-2Glc-H_2O]^-$	#	R
M53	56.73	Puerol B-sulfate	$C_{18}H_{16}O_8S$	391.0498 $[M-H]^-$	1.25	(−)311.0925 $[M-H-SO_3]^-$, 267.1026 $[M-H-SO_3-CO_2]^-$, 252.0788 $[M-H-SO_3-C_2H_3O_2]^-$	SUL	G
P36	57.64	Chikusetsusaponin FM1/ isomer	$C_{53}H_{92}O_{24}$	601.2976 $[M+2HCOO]^{2-}$	0.783	(−)1111.5939 $[M-H]^-$, 817.4984 $[M-H-Xyl/Api-Glc]^-$, 799.4854 $[M-H-Xyl/Api-Glc-H_2O]^-$, 637.4346 $[M-H-Xyl/Api-2Glc-H_2O]^-$	#	R
P37	58.81	Mal-G Rg1/isomer	$C_{45}H_{74}O_{17}$	885.4858 $[M-H]^-$	0.583	(−)781.4831 $[M-H-C_3H_2O_3-H_2O]^-$, 637.4350 $[M-H-C_3H_2O_3-Glc]^-$, 619.4228 $[M-H-C_3H_2O_3-Glc-H_2O]^-$, 475.3800 $[M-H-C_3H_2O_3-2Glc]^-$	#	R
P38	59.82	Unknown	$C_{13}H_{14}O_4$	235.0962 $[M+H]^+$	−1.214	(+)217.0860 $[M+H-H_2O]^+$, 207.1012 $[M+H-CO]^+$, 193.0493 $[M+H-C_3H_6]^+$, 179.0336 $[M+H-C_4H_8]^+$, 157.0647 $[M+H-C_2H_6O_3]^+$	#	C
P39	60.04	Unknown G	$C_{54}H_{92}O_{24}$	607.2976 $[M+2HCOO]^{2-}$	0.775	(−)1123.5961 $[M-H]^-$, 962.5426 $[M-H-C_6H_9O_5]^-$, 799.4909 $[M-H-2Glc]^-$, 781.4750 $[M-H-2Glc-H_2O]^-$, 619.4219 $[M-H-3Glc-H_2O]^-$	#	R
M54	60.07	Unknown GlcA	$C_{18}H_{26}O_9$	385.1507 $[M-H]^-$	0.765	(−)209.1179 $[M-H-GlcA]^-$, 165.1275 $[M-H-GlcA-CO_2]^-$	GlcA	C
P40	61.26	Genkwanin-5-*O*-primeveroside	$C_{27}H_{30}O_{14}$	579.1703 $[M+H]^+$	−0.918	(+)447.1256 $[M+H-Xyl]^+$, 285.0753 $[M+H-Xyl\ -Glc]^+$	#	G
P41	61.66	Unknown G	$C_{54}H_{92}O_{24}$	607.2977 $[M+2HCOO]^{2-}$	0.94	(−)1123.5895 $[M-H]^-$, 961.5399 $[M-H-Glc]^-$, 799.4846 $[M-H-2Glc]^-$, 781.4771 $[M-H-2Glc-H_2O]^-$, 637.4312 $[M-H-3Glc]^-$	#	R

Table 1 (continued)

No.	Rt (min)	Identification	Formula molecular	Precursor ions (*m/z*)	Error (ppm)	MS/MS	Metabolic pathway	Resource
M56	61.81	Unknown cysteine	$C_{15}H_{25}O_4NS$	316.1573 $[M+H]^+$	−1.283	(+)299.1306 $[M+H–NH_3]^+$, 270.1518 $[M+H–CH_2O_2]^+$, 195.1378 $[M+H–Cys]^+$, 177.1273 $[M+H–C_3H_7O_2NS-H_2O]^+$, 149.1324 $[M+H–C_3H_7O_2NS-CH_2O_2]^+$	Cys	C
P42	61.83	Unknown	$C_{21}H_{20}O_{10}$	431.0984 $[M-H]^-$	0.07	(−)269.0411 $[M-H–Glc]^-$, 268.0378 $[M-2H–Glc]^-$, 253.0500 $[M-H–Glc-O]^-$	#	D
P43	61.93	Unknown	$C_{16}H_{10}O_7$	313.0356 $[M-H]^-$	0.716	(−)298.0120 $[M-H–CH_3]^-$, 269.0457 $[M-H–CO_2]^-$	#	D
P44	62.10	Unknown G	$C_{54}H_{94}O_{24}$	608.3053 $[M+2HCOO]^{2-}$	0.568	(−)1125.6071 $[M-H]^-$, 963.5552 $[M-H–Glc]^-$, 801.4987 $[M-H–2Glc]^-$, 783.4926 $[M-H–2Glc–H_2O]^-$, 639.4543 $[M-H–3Glc]^-$	#	R
M57	62.19	Chrysophanol-sulfate	$C_{15}H_{10}O_7S$	333.0075 $[M-H]^-$	0.16	(−)253.0504 $[M-H–SO_3]^-$	SUL	D
M58	62.20	Emodin-GlcA	$C_{21}H_{18}O_{11}$	445.0777 $[M-H]^-$	0.147	(−)269.0456 $[M-H–GlcA]^-$, 225.0560 $[M-H–GlcA–CO_2]^-$	GlcA	D
M59	62.38	Chrysophanol-GlcA	$C_{21}H_{18}O_{10}$	429.0826 $[M-H]^-$	−0.279	(−)253.0508 $[M-H–GlcA]^-$	GlcA	D
M60	62.43	Unknown sulfate	$C_{13}H_{16}O_7S$	315.0547 $[M-H]^-$	0.963	(−)235.0972 $[M-H–SO_3]^-$, 220.0736 $[M-H–SO_3–CH_3]^-$, 191.1069 $[M-H–SO_3–CO_2]^-$, 176.0831 $[M-H–SO_3–C_2H_3O_2]^-$	SUL	C
M61	62.82	Unknown G	$C_{53}H_{92}O_{23}$	593.3003 $[M+2HCOO]^{2-}$	1.059	(−)1095.5964 $[M-H]^-$, 963.5530 $[M-H–Xyl]^-$, 801.4943 $[M-H–Xyl–Glc]^-$, 783.4885 $[M-H–Xyl–Glc–H_2O]^-$, 639.4460 $[M-H–Xyl–2Glc]^-$	deGlc	–
M62	64.51	Chrysophanol-GlcA	$C_{21}H_{18}O_{10}$	429.0827 $[M-H]^-$	−0.046	(−)253.0507 $[M-H–GlcA]^-$, 225.0545 $[M-H–GlcA–CO]^-$	GlcA	D
P45	64.67	Unknown G	$C_{48}H_{76}O_{21}$	987.4809 $[M-H]^-$	0.271	(−)925.4819 $[M-H–CH_2O_3]^-$, 779.4310 $[M-H–CH_2O_3-Rha]^-$, 661.3589 $[M-H–CH_2O_3-RhA–C_5H_{10}O_3]^-$, 485.3268 $[M-H–CH_2O_3-Rha–Glc–Xyl/Api]^-$	#	–

Table 1 (continued)

No.	Rt (min)	Identification	Formula molecular	Precursor ions (*m/z*)	Error (ppm)	MS/MS	Metabolic pathway	Resource
–	67.94	Puerol B	$C_{18}H_{16}O_5$	311.0928 $[M-H]^-$	0.974	(−)296.0688 $[M-H-CH3]^-$, 267.1027 $[M-H-CO_2]^-$, 252.0790 $[M-H-C_2H_3O_2]^-$, 205.0500 $[M-H-C_7H_6O]^-$	–	G
P46	68.04	G Ra0/Quinquenoside V	$C_{60}H_{102}O_{28}$	680.3264 $[M+2HCOO]^{2-}$	0.465	(−)1269.6372 $[M-H]^-$, 1107.5963 $[M-H-Glc]^-$, 945.5424 $[M-H-2Glc]^-$, 783.4895 $[M-H-3Glc]^-$, 621.4354 $[M-H-4Glc]^-$	#	R
–	68.4	Unknown	$C_{19}H_{18}O_6$	341.1032 $[M-H]^-$	0.406	(−)326.0798 $[M-H-CH_3]^-$, 297.1132 $[M-H-CO_2]^-$, 282.0897 $[M-H-C_2H_3O_2]^-$, 267.0664 $[M-H-C_3H_6O_2]^-$, 253.0504 $[M-H-C_4H_8O_2]^-$	–	G
P47	68.93	G ROA	$C_{54}H_{86}O_{24}$	581.2714 $[M-CO_2]^{2-}$	0.835	(−)1117.5370 $[M-H]^-$, 793.4373 $[M-H-2Glc]^-$, 613.3748 $[M-H-3Glc-H_2O]^-$, 455.3521 $[M-H-4GlC-GlcA]^-$	#	R
M63	69	Physcion-GlcA	$C_{22}H_{20}O_{11}$	459.0934 $[M-H]^-$	0.251	(−)283.0612 $[M-H-GlcA]^-$, 268.0370 $[M-H-GlcA-CH_3]^-$, 240.0417 $[M-H-GlcA-C_2H_3O]^-$	GlcA	D
P48	69.55	G Ra3/isomer	$C_{59}H_{100}O_{27}$	1285.6425 $[M+HCOO]^-$	-3.43	(−)1239.6393 $[M-H]^-$, 1107.5951 $[M-H-Xyl]^-$, 1077.5861 $[M-H-Glc]^-$, 945.5454 $[M-H-Glc-Xyl]^-$, 783.4919 $[M-H-2Glc-Xyl]^-$, 621.4357 $[M-H-3Glc-Xyl]^-$	#	R
M64	69.97	Unknown G	$C_{59}H_{98}O_{28}$	649.3084 $[M+CO_2]^{2-}$	1.088	(−)1253.6241 $[M-H]^-$, 1091.5645 $[M-H-Glc]^-$, 1074.5599 $[M-H-2Glc]^-$	deGlc	R
P49	70	G Rf*	$C_{42}H_{72}O_{14}$	845.4912 $[M+HCOO]^-$	0.935	(−)799.4850 $[M-H]^-$, 637.4318 $[M-H-Glc]^-$, 475.3792 $[M-H-2Glc]^-$	#	R
M65	70.65	Physcion-GlcA	$C_{22}H_{20}O_{11}$	459.0935 $[M-H]^-$	0.469	(−)283.0611 $[M-H-GlcA]^-$, 268.0372 $[M-H-GlcA-CH_3]^-$, 240.0413 $[M-H-GlcA-C_2H_3O]^-$	GlcA	D
M66	70.82	Emodin-GlcA	$C_{21}H_{18}O_{11}$	445.0777 $[M-H]^-$	0.147	(−)269.0456 $[M-H-GlcA]^-$, 241.0494 $[M-H-GlcA-CO]^-$, 225.0551 $[M-H-CO_2]^-$	GlcA	D

Table 1 (continued)

No.	Rt (min)	Identification	Formula molecular	Precursor ions (*m/z*)	Error (ppm)	MS/MS	Metabolic pathway	Resource
M67	70.87	26or27-carboxy PPT	$C_{30}H_{50}O_6$	505.3540 $[M-H]^-$	1.064	(−)461.3635 $[M-H-CO_2]^-$, 435.2762 $[M-H-C_5H_{10}]^-$, 391.2855 $[M-H-CO_2-C_5H_{10}]^-$, 373.2785 $[M-H-C_6H_{10}O_2-H_2O]^-$	Hydrogenation+hydroxylation	R
P50	71.17	G Ra0/Quinquenoside V	$C_{60}H_{102}O_{28}$	680.3264 $[M+2HCOO]^{2-}$	4.782	(−)1269.6421 $[M-H]^-$, 1107.5963 $[M-H-Glc]^-$, 945.5436 $[M-H-2Glc]^-$, 783.4826 $[M-H-3Glc]^-$, 621.4406 $[M-H-4Glc]^-$	#	R
P51	71.24	5,6-Didehydroginsenoside Rb1	$C_{54}H_{90}O_{23}$	598.2925 $[M+2HCOO]^{2-}$	1.092	(−)1105.5836 $[M-H]^-$, 943.5303 $[M-H-Glc]^-$, 781.4724 $[M-H-2Glc]^-$, 619.4205 $[M-H-3Glc]^-$, 457.3666 $[M-H-4Glc]^-$	#	R
P52	71.51	G F3/F5/N R2	$C_{41}H_{70}O_{13}$	815.4803 $[M+HCOO]^-$	0.559	(−)769.4737 $[M-H]^-$, 637.4323 $[M-H-Ara/Xyl]^-$, 475.3795 $[M-H-Ara/Xyl-Glc]^-$	#	R
P53	71.72	G Ra2	$C_{58}H_{98}O_{26}$	1255.6320 $[M+HCOO]^-$	−0.665	(−)1209.6274 $[M-H]^-$, 1077.5847 $[M-H-Xyl]^-$, 1047.5724 $[M-H-Glc]^-$, 945.5394 $[M-H-Xyl-Ara]^-$, 915.5228 $[M-H-Glc-Xyl]^-$, 783.4890 $[M-H-Xyl-Ara-Glc]^-$, 621.4404 $[M-H-Xyl-Ara-2Glc]^-$, 459.3863 $[M-H-Xyl-Ara-3Glc]^-$	#	R
P54	72.03	G Ra3/isomer	$C_{59}H_{100}O_{27}$	1285.6425 $[M+HCOO]^-$	1.138	(−)1239.6375 $[M-H]^-$, 1107.5969 $[M-H-Xyl]^-$, 1077.5861 $[M-H-Glc]^-$, 945.5433 $[M-H-Glc-Xyl]^-$, 783.4883 $[M-H-2Glc-Xyl]^-$, 621.4386 $[M-H-3Glc-Xyl]^-$	#	R
P55	72.09	G Rb1*	$C_{54}H_{92}O_{23}$	1153.6007 $[M+HCOO]^-$	−0.382	(−)1107.5957 $[M-H]^-$, 945.5425 $[M-H-Glc]^-$, 783.4901 $[M-H-2Glc]^-$, 621.4375 $[M-H-3Glc]^-$, 459.3852 $[M-H-4Glc]^-$	#	R

Table 1 (continued)

No.	Rt (min)	Identification	Formula molecular	Precursor ions (*m/z*)	Error (ppm)	MS/MS	Metabolic pathway	Resource
M68	72.4	Unknown G	$C_{61}H_{96}O_{27}$	652.3026 $[M+CO_2]^{2-}$	0.289	(−)1259.6073 $[M-H]^-$, 1097.5533 $[M-H-Glc]^-$, 1079.5382 $[M-H-Glc-H_2O]^-$, 935.5010 $[M-H-2Glc]^-$, 784.4910 $[M-H-2Glc\text{-}Xyl/ArA-H_2O-H]^-$, 621.4387 $[M-H-3Glc\text{-}Xyl/ArA-H_2O]^-$, 459.3857 $[M-H\text{-}4Glc\text{-}Xyl/ArA-H2O]^-$	deGlc	–
P56	72.64	Mal-G Rb1	$C_{57}H_{94}O_{26}$	1193.5958 $[M-H]^-$	−0.214	1149.6089 $[M-H-CO_2]^-$, 1107.5958 $[M-H-C_3H_2OH_2O_3]^-$, 945.5434 $[M-H-C_3H_2O_3-Glc]^-$, 783.4905 $[M-H-C_3H_2O_3-2Glc]^-$, 621.4390 $[M-H-C_3H_2O_3-3Glc]^-$, 459.3852 $[M-H-C_3H_2O_3-4Glc]^-$	#	R
P57	72.66	Hydroxyligustilide	$C_{12}H_{14}O_3$	207.1013 $[M+H]^+$	−1.308	(+)189.0908 $[M+H-H_2O]^+$, 161.0959 $[M+H-CH_2O_2]^+$, 151.0388 $[M+H-C_4H_8]^+$	#	C
P58	72.95	Rc*	$C_{53}H_{90}O_{22}$	1123.5899 $[M+HCOO]^-$	−0.235	(−)1077.5841 $[M-H]^-$, 945.5420 $[M-H-Ara]^-$, 915.5231 $[M-H-Glc]^-$, 783.4896 $[M-H-Ara-Glc]^-$, 621.4369 $[M-H-Ara-2Glc]^-$, 459.3833 $[M-H-Ara-3Glc]^-$	#	R
P59	72.95	Rg2*	$C_{42}H_{72}O_{13}$	829.4953 $[M+HCOO]^-$	−0.602	(−)783.4898 $[M-H]^-$, 637.4338 $[M-H-Rha]^-$, 619.4248 $[M-H-Rha-H_2O]^-$, 475.3795 $[M-H-Rha-Glc]^-$	#	R
P60	72.98	G Ra1	$C_{58}H_{98}O_{26}$	1255.6322 $[M+HCOO]^-$	−0.126	(−)1209.6267 $[M-H]^-$, 1077.5839 $[M-H-Xyl]^-$, 1047.5719 $[M-H-Glc]^-$, 945.5406 $[M-H-Xyl-Ara]^-$, 915.5331 $[M-H-Xyl-Glc]^-$, 783.4900 $[M-H-Xyl-Ara-Glc]^-$, 621.4407 $[M-H-Xyl-Ara-2Glc]^-$, 459.3873 $[M-H-Xyl-Ara-3Glc]^-$	#	R
P61	73.38	G Rh1	$C_{36}H_{62}O_9$	683.4375 $[M+HCOO]^-$	−0.126	(−)637.4302 $[M-H]^-$, 475.3787 $[M-H-Glc]^-$	#	R

Table 1 (continued)

No.	Rt (min)	Identification	Formula molecular	Precursor ions (*m/z*)	Error (ppm)	MS/MS	Metabolic pathway	Resource
P62	73.39	Mal-G Rc	$C_{56}H_{92}O_{25}$	1163.5853 $[M-H]^-$	−0.164	(−)1119.5996 $[M-H-CO_2]^-$, 1077.5840 $[M-H-C_3H_2O_3]^-$, 945.5415 $[M-H-C_3H_2O_3-Ara]^-$, 897.5140 $[M-H-C_3H_4O_4-Glc]^-$, 783.4896 $[M-H-C_3H_2O_3-Ara-Glc]^-$, 621.4375 $[M-H-C_3H_2O_3-Ara-2Glc]^-$, 459.3855 $[M-H-C_3H_2O_3-Ara-3Glc]^-$	#	R
P63	73.66	G Ro	$C_{48}H_{76}O_{19}$	955.4904 $[M-H]^-$	−0.422	(−)793.4382 $[M-H-Glc]^-$, 775.4258 $[M-H-Glc-H_2O]^-$, 613.3747 $[M-H-2Glc-H_2O]$-, 569.3857 $[M-H-2Glc-H_2O-CO_2]^-$, 523.3796 $[M-H-2Glc-H_2O-CO_2-CH_2O_2]^-$, 455.3546 $[M-H-2Glc-GlcA]^-$	#	R
P64	73.7	G Rb2*	$C_{53}H_{90}O_{22}$	1123.5902 $[M+HCOO]^-$	−0.335	(−)1077.5844 $[M-H]^-$, 945.5421 $[M-H-Ara]^-$, 915.5310 $[M-H-Glc]^-$, 783.4901 $[M-H-Ara-Glc]^-$, 621.4379 $[M-H-Ara-2Glc]^-$, 459.3845 $[M-H-Xyl-Ara-3Glc]^-$	#	R
M69	73.93	Methyl-Rhein	$C_{16}H_{10}O_6$	297.0403 $[M-H]^-$	−0.543	(−)282.0533 $[M-H-CH3]^-$, 253.0504 $[M-H-CO_2]^-$(+)299.0911 $[M+H]^+$, 284.0676 $[M+H-CH3]^+$	Methyl	D
P65	74.1	Mal-G Rb2	$C_{56}H_{92}O_{25}$	1163.5853 $[M-H]^-$	−0.164	(−)1119.6003 $[M-H-CO_2]^-$, 1077.5841 $[M-H-C_3H_2O_3]^-$, 945.5438 $[M-H-C_3H_2O_3-Ara]^-$, 897.5140 $[M-H-C_3H_4O_4-Glc]^-$, 783.4891 $[M-H-C_3H_2O_3-Ara-Glc]^-$, 621.4366 $[M-H-C_3H_2O_3-Ara-2Glc]^-$, 459.3838 $[M-H-C_3H_2O_3-Ara-3Glc]^-$	#	R

Table 1 (continued)

No.	Rt (min)	Identification	Formula molecular	Precursor ions (*m/z*)	Error (ppm)	MS/MS	Metabolic pathway	Resource
P66	74.37	Mal-G Rb1	$C_{56}H_{94}O_{24}$	620.3048 $[M+2HCOO]^{2-}$	−0.249	(−)1149.6057 $[M-H]^-$, 1107.5955 $[M-H-C_2H_2O]^-$, 1089.5837 $[M-H-C_2H_4O_2]^-$, 945.5412 $[M-H-C_2H_2O-Glc]^-$, 927.5333 $[M-H-C_2H_4O_2\text{-}Glc]^-$, 783.4889 $[M-H-C_2H_2O-2Glc]^-$, 765.4812 $[M-H-C_2H_4O_2-2Glc]^-$, 621.4319 $[M-H-C_2H_2O\text{-}3Glc]^-$	#	R
P67	75.26	G Rd*	$C_{48}H_{82}O_{18}$	991.5485 $[M+HCOO]^-$	0.184	(−)945.5425 $[M-H]^-$, 783.4899 $[M-H-Glc]^-$, 765.4801 $[M-H-Glc-H_2O]^-$, 621.4371 $[M-H-2Glc]^-$, 603.4243 $[M-H-2Glc-H_2O]^-$, 459.3846 $[M-H-3Glc]^-$	#	R
P68	75.5	28-Deglucosylchikusetsusaponin V	$C_{42}H_{66}O_{14}$	793.4382 $[M-H]^-$	0.278	(−)631.3852 $[M-H-Glc]^-$, 613.3796 $[M-H-Glc-H_2O]^-$, 569.3843 $[M-H-Glc-CH_2O_3]^-$, 455.3551 $[M-H-Glc-GlcA]^-$	#	R
P69	75.6	Mal-G Rd/isomer	$C_{51}H_{84}O_{21}$	1031.5432 $[M-H]^-$	−0.031	(−)987.5482 $[M-H-CO_2]^-$, 945.5424 $[M-H-C_3H_2O_3]^-$, 783.4890 $[M-H-C_3H_2O_3-Glc]^-$, 765.4800 $[M-H-C_3H_2O_3-H_2O-Glc]^-$, 621.4363 $[M-H-C_3H_2O_3-2Glc]^-$, 459.3834 $[M-H-C_3H_2O_3\text{-}3Glc]^-$	#	R
P70	75.87	Aloe emodin*	$C_{15}H_{10}O_5$	269.0454 $[M-H]^-$	−0.545	(−)240.0423 $[M-H-CHO]^-$	#	D
P71	77.7	N Fe	$C_{47}H_{80}O_{17}$	961.5377 $[M+HCOO]^-$	−0.055	(−)915.5319 $[M-H]^-$, 783.4901 $[M-H-Ara]^-$, 621.4376 $[M-H-Ara-Glc]^-$, 459.3848 $[M-H-Ara-2Glc]^-$	#	R
P72	77.77	Rhein*	$C_{15}H_8O_6$	283.0247 $[M-H]^-$	−0.393	(−)257.0454 $[M-H-CO+2H]^-$, 239.0347 $[M-H-CO_2]^-$, 227.0345 $[M-H-2CO]^-$	#	D

Table 1 (continued)

No.	Rt (min)	Identification	Formula molecular	Precursor ions (*m/z*)	Error (ppm)	MS/MS	Metabolic pathway	Resource
M70	78.65	Unknown G	$C_{60}H_{102}O_{26}$	664.3208 $[M+2HCOO]^{2-}$	0.295	(−)1089.5848 $[M-Xyl]^-$, 945.5419 $[M-H-2Xyl]^-$, 927.5365 $[M-H-Xyl-Glc]^-$, 783.4910 $[M-H-2Xyl-Glc]^-$, 622.4380 $[M-2Xyl-2Glc]^-$	deGlc	–
M71	79.16	Unknown G	–	649.3159 $[M-X]^{2-}$	–	(−)1059.5763 $[M-X]^-$, 927.5351 $[M-X-Rha/Xyl]^-$, 783.4879 $[M-X-Rha/Xyl]^-$, 765.4823 $[M-X-Rha/Xyl-C_6H_8O_4]^-$, 621.4365 $[M-X-Rha/Xyl-2C_6H_8O_4]^-$, 459.3850 $[M-X-Rha/Xyl-2C_6H_8O_4-Glc]^-$	deGlc	–
P73	79.76	G F2/isomer	$C_{42}H_{72}O_{13}$	829.4963 $[M+HCOO]^-$	0.971	(−)621.4380 $[M-H-Glc]^-$, 459.3832 $[M-H-2Glc]^-$	#	R
M72	80.21	G F4	$C_{42}H_{70}O_{12}$	811.4856 $[M+HCOO]^-$	0.826	(−)765.4771 $[M-H]^-$, 619.4213 $[M-H-Rha]^-$, 457.3720 $[M-H-Rha-Glc]^-$	deGlc	R
P74	80.8	Chikusetsusaponin Iva	$C_{42}H_{66}O_{14}$	793.4383 $[M-H]^-$	0.404	(−)731.4357 $[M-H-CH_2O_3]^-$, 613.3748 $[M-H-Glc-H_2O]^-$, 569.3835 $[M-H-CH_2O_3\text{-}Glc]^-$, 523.3805 $[M-H-CH_2O_3\text{-}Glc-CH_2O_2]^-$, 455.3525 $[M-H-GlC-GlcA]^-$	#	R
M73	81.04	Unknown G	–	1121.5904 $[M-H]^-$	–	(−)927.5319 $[M-X]^-$, 765.4771 $[M-X\text{-}Glc]^-$, 621.4361 $[M-X\text{-}Glc-C_{10}H_8O]^-$, 459.3875 $[M-X-2Glc-C_{10}H_8O]^-$	deGlc	–
P75	81.66	G Rg3*	$C_{42}H_{72}O_{13}$	829.4962 $[M+HCOO]^-$	0.85	(−)783.4906 $[M-H]^-$, 621.4374 $[M-H-Glc]^-$, 459.3852 $[M-H-2Glc]^-$	#	R
M74	82.9	G Mc/Mx/Y	$C_{41}H_{70}O_{12}$	799.4855 $[M+HCOO]^-$	0.713	(−)753.4835 $[M-H]^-$, 621.4395 $[M-H-Ara]^-$, 459.3835 $[M-H-Ara]^-$	deGlc	R
P76	83.82	Emodin*	$C_{15}H_{10}O_5$	269.0455 $[M-H]^-$	−0.173	(−)241.0498 $[M-H-CO]^-$, 225.0555 $[M-H-CO_2]^-$	#	D

Table 1 (continued)

No.	Rt (min)	Identification	Formula molecular	Precursor ions (*m/z*)	Error (ppm)	MS/MS	Metabolic pathway	Resource
P77	83.93	28-Desglucosylchikusetsu-saponin IVa	$C_{36}H_{56}O_9$	631.3853 $[M-H]^-$	0.227	(−)555.3665 [M−H–$C_2H_4O_3$]$^-$, 455.3519 [M−H–GlcA]$^-$	#	R
P78	84.93	Oleanolic acid 3-*O*-Glc	$C_{36}H_{58}O_8$	663.4119 $[M+HCOO]^-$	0.797	(−)455.3532 [M−H–Glc]$^-$	#	R
P79	86.21	G Rg31/Rg5/Rk1/Rz1	$C_{42}H_{70}O_{12}$	811.4858 $[M+HCOO]^-$	1.072	(−)765.4822 [M−H]$^-$, 603.4264 [M−H–Glc]$^-$, 221.0665 [Glc–Glc]$^-$	#	R
M75	86.21	G C-K	$C_{36}H_{62}O_8$	667.4432 $[M+HCOO]^-$	0.792	(−)459.3830 [M−H–Glc]$^-$, 395.3698 [M−H–Glc–CH_4O_3]$^-$	deGlc	R

deGlc deglycosylation; hydrolysis hydrogenation; hydroxylation; *Cys* cysteine; *N* notoginsenoside; *G* ginsenoside; *NAcCys N*-acetylcysteine; *Mal* malonyl; *Ac* acetyl; *PPT* protopanaxtriol; *Xyl* xylose; *Glc* glucose; *Api* apiose; *Ara* arabinose; *Rha* rhamnose; *R Radix Ginseng*; *C Rhizoma Ligustici Chuanxiong*; *D Radix et Rhizoma Rhei*; *G Radix Puerariae*

#Prototype

* Confirmed by reference

–: no/unknown

P75 were identified as Rg1, Re, Rf, Ra2, Ra3/isomer, Rb1, Rc, Rg2, Ra1, Rh1, Rd, and Rg3, respectively. P39 displayed molecular $[M+2HCOO]^{2-}$ ions at *m/z* 607.2963, and the molecular formula was determined to be $C_{54}H_{92}O_{24}$. In the MS/MS spectrum, the fragment ions at *m/z* 962.5426 $[M-H-C_6H_9O_5]^-$, 799.4909 $[M-H-2Glc]^-$, 781.4750 $[M-H-2Glc-H_2O]^-$, and 619.4219 $[M-H-3Glc-H_2O]^-$ were obtained. The mass spectrum is shown in Fig. 2, showing that P39 contains 4 glucose groups, with at least two glucose groups attached. There was no report that P39 was isolated in ginseng herbs. Based on the fragment peak of P39 at *m/z* 475.7160, we judged the peak to be of the PPT type.

M67 showed the $[M-H]^-$ ion at *m/z* 505.3540 and yielded product ions at *m/z* 461.3635, 435.2762, 391.2855 and *m/z* 373.2785, which were formed by the losses of CO_2^-, $C_5H_{10}^-$, CO_2^- and $C_5H_{10}^-$, $C_6H_{10}O_2^-$ and H_2O^-, respectively. Based on the relevant study [24]. M67 was tentatively identified as 26/27-carboxy PPT. M22, M64, M72, M74, and M75, which were discovered in the spectrum of the NMT decoction, were deduced to be metabolites. They were tentatively assigned as 25-hydroxyl-PPT-*O*-diglucoside, unknown triterpenoid saponins, ginsenoside F_4 [24], ginsenoside Mc/Mx/Y [25, 26], and ginsenoside C-K [24], respectively.

M22 displayed the $[M+HCOO]^-$ ion at *m/z* 863.5018 ($C_{42}H_{74}O_{15}$), which product daughter ions at *m/z* 655.4435 and *m/z* 493.3895 from the product ion spectrum demonstrated losses of $C_6H_8O_6^-$ and 2 $C_6H_8O_6^-$ from the precursor ion $[M-H]^-$, respectively. The low mass fragments produced the product ions at *m/z* 179.0552, 161.0443, and 119.0335. The MS^2 of M22 is shown in Fig. 3. The structure of M22 involved two unrelated groups of glucose. Aglycone was tentatively identified as 25-hydroxyl-PPT via the fragment ion at *m/z* 493.3886. Its possible molecular formula and structural formula were searched in the SciFinder database, compared with the relevant literature [27, 28], and determined that the glucose groups were linked triterpenoid saponins. However, this determination was inconsistent with the above inference. Thus, M22 might be a new triterpenoid saponin.

Ingredients Derived from Pueraria lobata (Willd.) Ohwi

Eight pueraria glycosides (2 prototype ingredients), thirty-two isoflavones (18 prototype components), one prototype compound flavonoid (genkwanin-5-*O*-primeveroside), and three unknown compositions were detected in rat urine of the NMT-dosed and pueraria-dosed groups after oral administration. Two of the twenty-one prototypes (P3 and P15) had no relevant literature to report. They were identified as mirificin-*O*-glucoside and methoxypuerarin

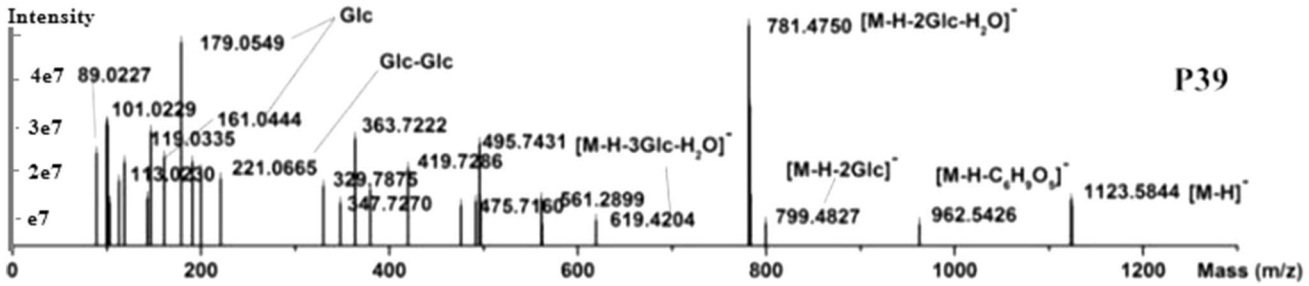

Fig. 2 MS/MS spectra of P39 with fragmentation peaks: *m/z* 962.5462, 799.4827, 781.4750, 179.0549, and 221.0665, with characteristic fragmentation peaks of *m/z* 475.7160, identified as protopanaxtriol type. *Glc* glucose

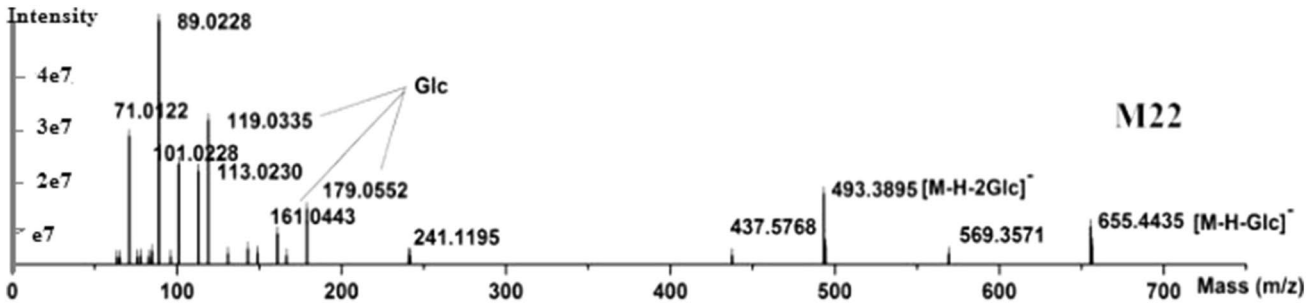

Fig. 3 MS/MS spectra of M22, showing the fragmentation peaks: *m/z* 655.4435, 493.3875, and 179.0052, tentatively assigned to a triterpenoid saponin. *Glc* glucose

according to the molecular ion peak and secondary cleavage patterns. Twenty-two metabolites involved 10 glucuronidation, 1 methoxylation, 8 sulfations, and 3 unknown metabolic reactions. In the urine of the rats dosed with compound NMT, we found that the metabolic pathway of isoflavones was based on phase II metabolisms, including glucuronidation, sulfation, and methylation (for related metabolic pathways, see Electronic Supplementary Material Fig. S5). However, the specific location of the glucuronidation, sulfation, and methylation was not yet determined. The metabolite compounds of pueraria were detected the first in the NMT-dosed group. Most compounds in the urine from the NMT-dosed and pueraria-dosed groups displayed strong signals at 0–8 h and 8–12 h. In addition, it can be detected after 8–12 h from NMT-dosed group and eliminated slowly. It showed that the Chinese medicine compounds contributed to an extension of the therapeutic time period.

P9 showed $[M+H]^+$ at *m/z* 417.1175 in the positive ion mode. The characteristic fragment ions at *m/z* 399.1072, 297.0755, and 267.0652 shown in the product ion spectrum identified the loss of H_2O, $C_4H_8O_4$, and $C_5H_{10}O_5$ from the precursor ion $[M+H]^+$, respectively. In addition, the retention time of P9 was compared with the retention time and MS^2 of the Ref. [29]. Therefore, P9 was determined to be puerarin. P6 and P11 showed diagnostic neutral losses 0f H_2O, $C_4H_8O_4$, and $C_5H_{10}O_5$ from the precursor ion $[M+H]^+$. Based on the related Ref. [29], P6 and P11 were identified as 3′-hydroxypuerarin and 3′-methoxypuerarin, respectively.

Among the metabolite components, M3 comprised the same aglycone, puerarin (P9), yielded a series of characteristic ions of puerarin at *m/z* 399.1072, 381.0964, 297.0755, and 267.0652, and displayed a mass 176 Da higher than P9 ($[M-H]^-$ ion at *m/z* 417.1175). Therefore, M3 was identified as a glucuronidated conjugated products of P9. Thus, M3 was assigned as puerarin-*O*-glucuronide based on the literature [30]. Similarly, M1 and M9 were identified as puerarin-sulfate and puerarin-glucuronide, respectively.

M7 and M12, with retention times of 7.76 and 9.13 min, respectively, generated the different $[M-H]^-$ ions at *m/z* 607.1309 and 511.0553, respectively. Their molecular weights were higher (176 Da ($C_6H_8O_6$) and 80 Da (SO_3) than the molecular weight of P6 (3′-hydroxypuerarin). Therefore, M7 and M12 were identified as the glucuronide and sulfated conjugated products of P6, respectively. However, the position of the glucuronide and sulfated reaction site could not be confirmed in this present study.

M11 and M13 were, respectively, eluted at 8.66 and 9.59 min with the $[M-H]^-$ ions at *m/z* 525.0714 ($C_{22}H_{22}O_{13}S$) and 621.1461 ($C_{28}H_{30}O_{16}$), which were 80 Da (SO_3) and 176 Da ($C_6H_8O_6$) more than the ions of P11 (*m/z* 447.128), respectively. We deduced that sulfated and glucuronide conjugation occurred to P11. They showed

fragment ions at *m/z* 325.0722 in the MS/MS spectra, similar to the fragment ions of P11. Therefore, they were unambiguously identified as 3′-methoxypuerarin-sulfate and 3′-methoxypuerarin-glucuronide. However, the precise position of the sulfated and glucuronide reaction site still needed further confirmation.

Ingredients Derived from Ligusticum Chuanxiong Hort

Totally, 21 components from *Rhizoma Chuanxiong* were detected in the urine from the NMT-dosed and *Ligusticum chuanxiong Hort*-dosed groups, including four prototypes (ferulic acid, senkyunolide K/G, hydroxyligustilide, and a component of unknown composition), seven metabolites, and ten components of unknown composition (mainly phthalide senkyunolide and phenolic acids). Prototype and components from *Ligusticum chuanxiong Hort* showed intense signals at 0-8 h and 8–12 h. In addition, a few components can be detected after 12 h from *Ligusticum chuanxiong Hort*-dosed group. Over time, these signals weaken gradually or even disappeared. The metabolites were 4 cysteine conjugations, 6 glucuronidations, 1 hydrolysis of sulfation, 2 acetylcysteine conjugations, 3 sulfate conjugations, and 1 unknown metabolic pathway metabolite. For related metabolic pathways, see Electronic Supplementary Material Fig. S6. The fragmentation routes of cysteine conjugates show cleavage of the Ro'-S bond (loss of 121 Da and formation of the fragment at *m/z* 122 in the positive ion mode) or cleavage of the S CH_2 bond is observed, leading to a loss of 87 and/or 89 Da, as exemplified for Cys conjugated to boscalid. Upon collision, this NAcCys conjugate exhibits a neutral loss of 42 Da, i.e., a loss of ketene, which allows rapid identification of the acetylated molecule [31].

Most of the phenol components had abundant signal in the positive ion mode. There were two main forms of $[M+H]^+$ and $[M+Na]^+$ with an excimer ion peak, where the cleavage mode was mainly loss of H_2O (18 Da), CO (28 Da), and branched off ene. Based on above information and the related reference, P17 was identified as ferulic acid.

M52 showed $[M+H]^+$ ions at *m/z* 374.1629, revealing that the molecular formula of M52 was $C_{17}H_{27}O_6NS$. The ions could lose HCOOH, C_2H_5NO, and $C_5H_9NSO_3$ to form the fragments with *m/z* 328.1574, 315.1249, and *m/z* 211.1327. From the previous study [31], acetylcysteine conjugation could be inferred from the *m/z* 46.01 Da (HCOOH), 59.04 Da (C_2H_5NO), and 163.03 Da ($C_5H_9NSO_3$), the characteristics of loss of neutral molecules. Therefore, M52 was identified as the acetylcysteine conjugate of senkyunolide. M32 displayed the $[M+H]^+$ ion at *m/z* 330.1366, yielding a product ion at *m/z* 209.1170, which was formed by the loss of $C_3H_8NO_2S$ (121 Da) from the $[M+H]^+$ ion. In addition, M32 exhibited product ions at *m/z* 163.1140, 191.2090, and 209.1170, the characteristic ions of senkyunolide in the positive mode, demonstrating that it was a senkyunolide-related metabolite. From a previous study [32], M32 was tentatively identified as senkyunolide J/N cysteine.

The deprotonated molecule of *m/z* 369.0829 ($[M-H]^-$, M8) eluted at 7.80 min and was 176 Da ($C_6H_8O_6$) more than the deprotonated molecule of P17 (ferulic acid) detected in the urine samples. In addition, M8 showed fragment ions *m/z* 177.0544 and 145.0287 in the MS/MS spectra, which were similar to those of P17. Finally, M8 was tentatively assigned as the glucuronide conjugated metabolite of P17 on the basis of the above information.

Ingredients Derived from Unknown Sources

Comparing the compound urine, mass spectral data with single-drug prescriptions found 14 urine components of unknown origin. According to the secondary fragments, seven components were identified. M2, P1, M3, M4, M5, M34, and P29 were 3′-hydroxypuerarin-*O*-glucuronides, 3′-hydroxylpuerarin-*O*-glucoside (prototypes), puerarin-*O*-glucuronide, 3′-hydroxypuerarin-*O*-sulfate, 3′-methoxypuerarin-*O*-glucuronide, senkyunolide J/N cysteine conjugates, and isoswertisin-2′-*O*-xyloside (prototypes). The remaining peaks, M61, P45, M68, M70, M71, and M73, were initially assigned as triterpenoid saponins. P45 was a prototype component, and M68, M71, and M73 were of the protopanaxadiol type (according to the characteristics

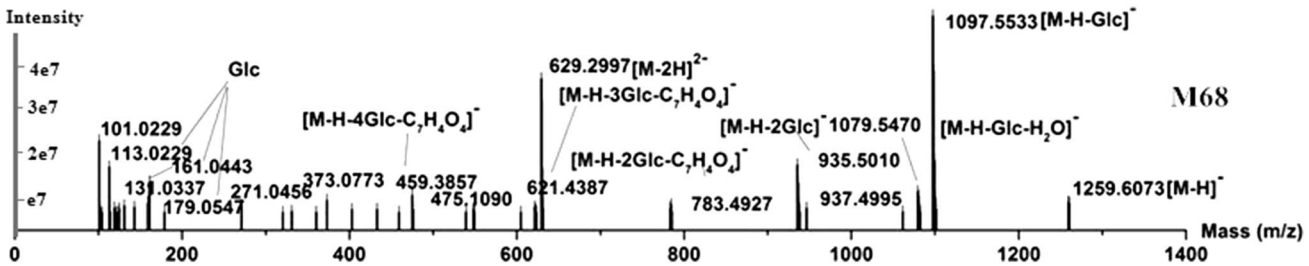

Fig. 4 MS/MS spectra of M68 showing $[M-H]^-$ ions at *m/z* 1259.603, yield fragmentation peaks: 1097.5533, 783.4972, 621.4387, 459.3857, tentatively assigned to a saponin compound

of the fragment ion at *m/z* 459.39), and M42 showed acetylcysteine conjugation.

M68 showed $[M+CO_2]^{2-}$ at *m/z* 652.3026 in the negative ion mode, manifesting that the molecular formula of M68 was $C_{61}H_{96}O_{27}$ and yielded product ions at *m/z* 1097.5533, 1079.5382, 935.5010, 784.4910, 621.4387, and 459.3857. MS^2 of M68 is shown in Fig. 4. The compound had not been found in the SciFinder database, so M68 might be a new saponin compound.

Discussion

Using HPLC-Q-Orbitrap and MetWorks™ software, abundant chemical components of NMT were tentatively identified. The assigned chemical components mainly were anthraquinones, triterpenoid saponins, isoflavones, puerosides, phthalides, and phenolic acid. Many compounds from *Radix et Rhizoma Rhei*, Panax ginseng C.A. Mey., *Pueraria lobata* (Willd.) Ohwi., and *Ligusticum chuanxiong Hort* presented different absorption trends and slower elimination rates in the urine from the NMT-dosed group compared with the urine from the single-dosed groups. The metabolites of rhubarb also displayed strong signals after 8–12 h in urine, while most metabolites displayed strong ion signals at 0.5 and 8 h in plasma [7]. It indicated that the metabolites of rhubarb were eliminated slower in urine than in plasma. Aloe emodin were detected in the urine, but was not found in the plasma [7]. It showed that aloe emodin is not absorbed into the blood, but with the urine excreted in vitro. Methylation conjugation of the metabolism pathway was found in the urine. The prototype components and metabolites of ginseng were rarely detected in the rat plasma [7], while an amount of them were found in the rat urine. Hydroxylated, hydrogenated, and hydrolyzed as major metabolism pathways had been found in the rat urine. It indicated that ginseng is rarely absorbed into the blood, metabolized in vivo, and then excreted with the urine. Ginsenoside Rg1, ginsenoside Rb1, ginsenoside Rb3, and ginsenoside Rc might be the most important constituents controlling the pharmacological effects of NMT by comparing 15 absorbed ingredients through principal component analysis [8]. However, the metabolic mechanism of ginseng still needs further study. The metabolites of pueraria also displayed strong signals after 8–12 h in urine. Mirificin-Glc and methoxypuerarin were first discovered in puerariae in urine. The prototype compound of 3′-hydroxypuerarin was detected in urine, but not found in plasma. 3′-methyoxy puerarin-6″-*O*-Glc was not detected in plasma [7], but found in urine. However, the metabolism of NMT in rat plasma and urine still needs further study. This result displayed that prescription compatibility in TCM could influence the absorption of a few components in urine and in plasma. In addition, because the concentration of metabolites in rat urine was low and was not favorable for detection, the rats were treated with high doses relative to humans. However, the metabolites of NMT in human urine require further investigation.

Metabolites or components observed in vivo might produce pharmacological bioactivities. The previous studies have showed that chrysophanol has anti-inflammation activity to protect mice from cerebral ischemic injury [33] and emodin exerts neuro-protective effects against glutamate-induced apoptosis in cerebral ischemia [34]. In addition, ginsenosides, such as Rg1, Re, Rd, and Rb1, can reportedly act as neuroprotectants through various mechanisms, including inducing the activating the PI3 K/Akt pathway [35], ameliorating lipid peroxidation [36], and protecting the integrity of the blood–brain barrier [37]. Moreover, 3′-methoxypuerarin could protect rats against cerebral ischemia–reperfusion injury [38]. Furthermore, senkyunolide I [39], ligustilide [40], and ferulic acid [41] from *L. Wallichiii* are active anti-cerebral ischemia substance. However, the pharmacological activities of more metabolites need more deeply study.

Conclusions

In this study, a rapid HPLC-Q-Orbitrap method was the first used for analyzing rat urinary metabolites after oral administration of NMT and its single herbs. Consequently, a total of 157 compounds, including 79 prototype compounds (70 of them had been identified) and 78 metabolites (61 of them had been tentatively identified) were detected in the NMT drug-containing group. Most of the ingredients were found in the urine during 0–8 h and 8–12 h periods; fewer ginsenosides were detected after 12 h. The results indicated that anthraquinone, triterpenoid saponins, isoflavones, puerarin glycosides, senkyunolide, and phenolic acids were potentially effective components of NMT. Glucuronidation and sulfation were the main metabolic pathways of *Radix et Rhizoma Rhei* and *Pueraria lobata (Willd.) Ohwi.*, two components of NMT. In addition to glucuronidation and sulfation, other conjugation reactions also occurred in the metabolisms of *Ligusticum chuanxiong Hort.* such as cysteine conjugation and acetylcysteine conjugation. Glucuronidation and sulfation metabolites of *Panax ginseng C.A. Mey.* had not been found, and fewer metabolites of *Panax ginseng C.A. Mey.* were detected, so the metabolic pathways had deglycosylated, hydroxylated, and hydrogenated hydrolysis. Many of the components identified in the urine from the single herb-dosed groups showed different eliminated rates from that detected in the urine from the NMT-dosed. Because of the complexity of the constituents in NMT, the origins and structures of some metabolites could not be definitely elucidated with the

current analytical methods. Therefore, this study provides useful information for the further study of the pharmacology and mechanism of action of NMT.

Compliance with Ethical Standards

Conflict of interest The authors declare that they have no conflict of interest.

Ethical approval All applicable international, national, and institutional guidelines for the care and use of animals were followed.

Funding This study was funded by 81274060 and 81473413.

References

1. Ren XQ, Li JS, Feng YM, Lu YQ (2004) Neuro-protective effect of NaoMaiTong to brain damage after focal cerebral ischemia reperfusion(I R)in the aged rats. China J Chin Mater Med 29:66–70 **(in Chinese)**
2. Li JS, Guo DM (2005) Clinical effect analysis of acute cerebral infarction treated by Naomaitong granules. China J Tradit Chin Med Pharm 20:563–565 **(in Chinese)**
3. Li JS, Gao JF, Zhou YL, Liu K (2006) Neuro-protective effect of Naomaitong to inflammatory cascade response after focal cerebral ischemia reperfusion in aged rats. China J Chin Mater Med 31:1804–1807 **(in Chinese)**
4. Liu K, Li JS, Gao JF, Yang XK, Zhou YL, Zhao YW, Liu ZG, Liu JX (2010) Effect of Naomaitong on cerebral angiogenesis and expressions of VEGF and VEGFR after cerebral ischemia/reperfusion in aged rats. China J Tradit Chin Med Pharm 12:2088–2092 **(in Chinese)**
5. Chen X, Yang YX, Wang SM, Wang ZH, Su ZB, Li JS, Liang SW (2012) Study on effects of extract in Naomaitong formula on cerebral ischemia–reperfusion model based on NMR metabolomics. Chin Tradit Herb Drugs 43:97–102 **(in Chinese)**
6. Wang SM, Li SF, Liang SW, Gao SJ, Li JS (2009) Separation and purification of Naomaitong granules by AB-8 macroporous absorption resin. Chin Tradit Patent Med 31:47–50 **(in Chinese)**
7. Rong YY, Feng SX, Wu CW, Wang SM, Liang SW, Liu DY (2016) LC-high-resolution-MS/MS analysis of chemical compounds in rat plasma after oral administration of Nao-Mai-Tong and its individual herbs. Biomed Chromatogr 13:1–13
8. Wu CW, Zhao L, Rong YY, Zhu GX, Liang SW, Wang SM (2016) The pharmacokinetic screening of multiple components of the NaoMai Tong formula in rat plasma by liquid chromatography tandem/mass spectrometry combined with pattern recognition method andits application to comparative pharmacokinetics. Pharm Biomed Anal 131:345–354
9. Zhang H, Zhang D, Ray K (2003) A software filter to remove interference ions from drug metabolites in accurate mass liquid chromatography/mass spectrometric analyses. Mass Spectrom 38:1110–1112
10. Song R, Xu L, Xu FG et al (2010) In vivo metabolism study of rhubarb decoction in rat using high-performance liquid chromatography with UV photodiode-array and mass-spectrometric detection: a strategy for systematic analysis of metabolites from traditional Chinese medicines in biological samples. Chromagr A 127:7144–7152
11. Wang M, Fu JF, Lv MY et al (2014) Effect of wine processing and acute blood stasis on the serum pharmacochemistry of rhubarb: a possible explanation for processing mechanism. Sep Sci 27:2499–2503
12. Jiang P, Liu RH, Dou SS et al (2009) Analysis of the constituents in rat plasma after oral administration of Shexiang Baoxin pill by HPLC-ESI-MS/MS. Biomed Chromatogr 23:1333–1343
13. Qian TX, Jiang ZH, Cai ZW (2006) High-performance liquid chromatography coupled with tandem mass spectrometry applied for metabolic study of ginsenoside Rb1 on rat. Anal Biochem 352:87–96
14. Kim U, Park MH, Kim DH et al (2013) Metabolite profiling of ginsenoside Re in rat urine and faeces after oral administration. Food Chem 136:1364–1369
15. Xu Q, Tan YJ, Su XJ, Luo WS (2009) Stuides on chemical constituents of *Rheum palmatum*. Chin Tradit Herb Drugs 40(4):536
16. Song R, Xu L, Xu FG, Li ZG, Dong H, Tian Y, Zhang Z (2010) In vivo metabolism study of rhubarb decoction in rat using high-performance liquid chromatography with UV photodiode-array and mass-spectrometric detection: a strategy for systematic analysis of metabolites from traditional Chinese medicines in biological samples. Chromagr A 127:7144–7152
17. Wu WJ, Hu N, Zhang QW, Li YP, Li P, Yan R, Wang YT (2014) In vitro glucuronidation of five rhubarb anthraquinones by intestinal and liver microsomes from humans and rats. Chem Biol Interact 219:18–27
18. Wu WJ, Yan R, Yao MC, Zhan Y, Wang YT (2014) Pharmacokinetics of anthraquinones in rat plasma after oral administration of a rhubarb extract. Biomed Chromatogr 28:564–572
19. Song R, Xu FG, Zhang ZJ, Liu Y, Dong HJ, Tian Y (2008) Structural elucidation of in vitro metabolites of emodin by liquid chromatography–tandem massspectrometry. Biomed Chromatogr 22:1230–1236
20. Koyama J, Takeuchi A, Morita I, Nishino Y, Shimizu M, Inoue M, Kobayashi N (2009) Characterization of emodin metabolites in Raji cells by LC–APCI-MS/MS. Med Chem 17:7493–7499
21. Qiu S, Yang WZ et al (2015) A green protocol for efficient discovery of novel natural compounds: characterization of new ginsenosides from the stems and leaves of Panax ginseng as a case study. Anal Chim Acta 893:65–76
22. Qi LW, Wang HY, Zhang H, Wang CZ, Li P, Yuan CS (2012) Diagnostic ion filtering to characterize ginseng saponins by rapid liquid chromatography with time-of-flight mass spectro- metry. Chromatogr A 1230:93–99
23. Wan JW, Wang CZ et al (2016) Determination of American ginseng saponins and their metabolites in human plasma, urine and feces samples by liquid chromatography coupled with quadrupole time-of-flight mass spectrometry. Chromatogr B 1015:62–73
24. He CY, Zhou DD, Li J, Han H, Ji G, Yang L, Wang Z (2014) Identification of 20(S)-protopanaxatriol metabolites in rats by ultra-performance liquid chromatography coupled with electrospray ionization quadrupole time-of-flight tandem mass spectrometry and nuclear magnetic resonance spectroscopy. Pharm Biomed Anal 88:497–500
25. Zhou SS, Xu JD et al (2014) Simultaneous determination of original, degraded ginsenosides and aglycones by ultra high performance liquid chromate- graphy coupled with quadrupole time-of-flight mass spectrometry for quantitative evaluation of Du-Shen-Tang, the decoction of ginseng. Molecules 19:4083–4104
26. Yang HY, Lee DY, Kyobin K, Kim JY, Kim SO, YooYH Sung SH (2015) Identification of ginsenoside markers from dry purified extract of Panax ginseng by a dereplication approach and UPLC–QTOF/MS analysis. Pharm Biomed Anal 109:91–104
27. Wu W, Qin QJ, Guo YY, Sun JH, Liu SY (2012) Studies on the chemical transformation of 20(S)-protopanaxatriol (PPT)-type ginsenosides R(e), R(g2), and R(f) using rapid resolution liquid chromatography coupled with quadruple-time-of-flight

mass spectrometry (RRLC-Q-TOF-MS). Agric Food Chem 60(40):10007–10014
28. Xing QQ, Liang T, Shen GB, Wang XL, Jin Y, Liang XM (2012) Comprehensive HILIC × RPLC with mass spectrometry detection for the analysis of saponins in *Panax notoginseng*. Analyst 137(9):2239–2249
29. Miao WJ, Wang Q, Bo T et al (2013) Rapid characterization of chemical constituents and rats metabolites of the traditional Chinese patent medicine Gegen–Qinlian–Wan by UHPLC/DAD/qTOF-MS. Pharm Biomed Anal 72:99–108
30. Yan Y, Chai CZ et al (2013) HPLC-DAD-Q-TOF-MS/MS analysis and HPLC quantitation of chemical constituents in traditional Chinese medicinal formula Ge-Gen Decoction. Pharm Biomed Anal 80:192–202
31. Levsen K, Schiebel HM, Behnke B et al (2005) Structure elucidation of phase II metabolites by tandem mass spectrometry: an overview. Chromatogr A 1067:55–72
32. Yan R, Ko NL, Li SL, Tam YK, Lin G (2008) Pharmacokinetics and metabolism of ligustilide, a major bioactive component in Rhizoma Chuanxiong, in the rat. Drug Metab Dispos 36:400–408
33. Zhang N, Zhang X, Liu X, Wang H, Xue J, Yu J et al (2014) Chrysophanol inhibits NALP3 inflammasome activation and ameliorates cerebral ischemia/reperfusion in mice. Mediat Inflamm. doi:10.1155/2014/370530
34. Ahn SM, Kim HN, Kim Y et al (2017) Emodin from *Polygonum multiflorum* ameliorates oxidative toxicity in HT22 cells and deficits in photothrombotic ischemia. J Ethnophamacol 188:13–20
35. Liu XY, Zhou XY, Hou JC, Zhu H et al (2015) Ginsenoside Rd promotes neurogenesis in rat brain after transient focal cerebral ischemia via activation of PI3 K/Akt pathway. Acta Pharmacol Sin 36:421–428
36. Zhou XM, Cao YL, Dou DQ (2006) Protective effect of ginsenoside-Re against cerebral ischemia/reperfusion damage in rats. Biol Pharm Bull 29:2502–2505
37. Chen W, Guo Y, Yang W, Zheng J, Tong W (2015) Protective effect of ginsenoside Rb1 on integrity of blood–brain barrier following cerebral ischemia. Exp Brain Res 233:2823–2831
38. Aras AB, Guven M, Akman T, Ozkan A et al (2015) Neuroprotective effects of daidzein on focal cerebral ischemia injury in rats. Neural Regen Res 10:146–152
39. Hu Y, Duan M, Liang S, Wang Y, Feng Y (2015) Senkyunolide I protects rat brain against focal cerebral ischemia–reperfusion injury by up-regulating p-Erk1/2, Nrf2/HO-1 and inhibiting caspase 3. Brain Res 1605:39–48
40. Peng B, Zhao P, Lu YP, Chen MM, Sun H, Wu XM, Zhou L (2013) Z-ligustilide activates the Nrf2/HO-1 pathway and protects against cerebral ischemia–reperfusion injury in vivo and in vitro. Brain Res 1520:168–177
41. Cheng CY, Su SY, Tang NY, Ho TY, Lo WY, Hsieh CL (2010) Ferulic acid inhibits nitric oxide-induced apoptosis by enhancing GABA(B1) receptor expression in transient focal cerebral ischemia in rats. Acta Pharmacol Sin 31:889–899